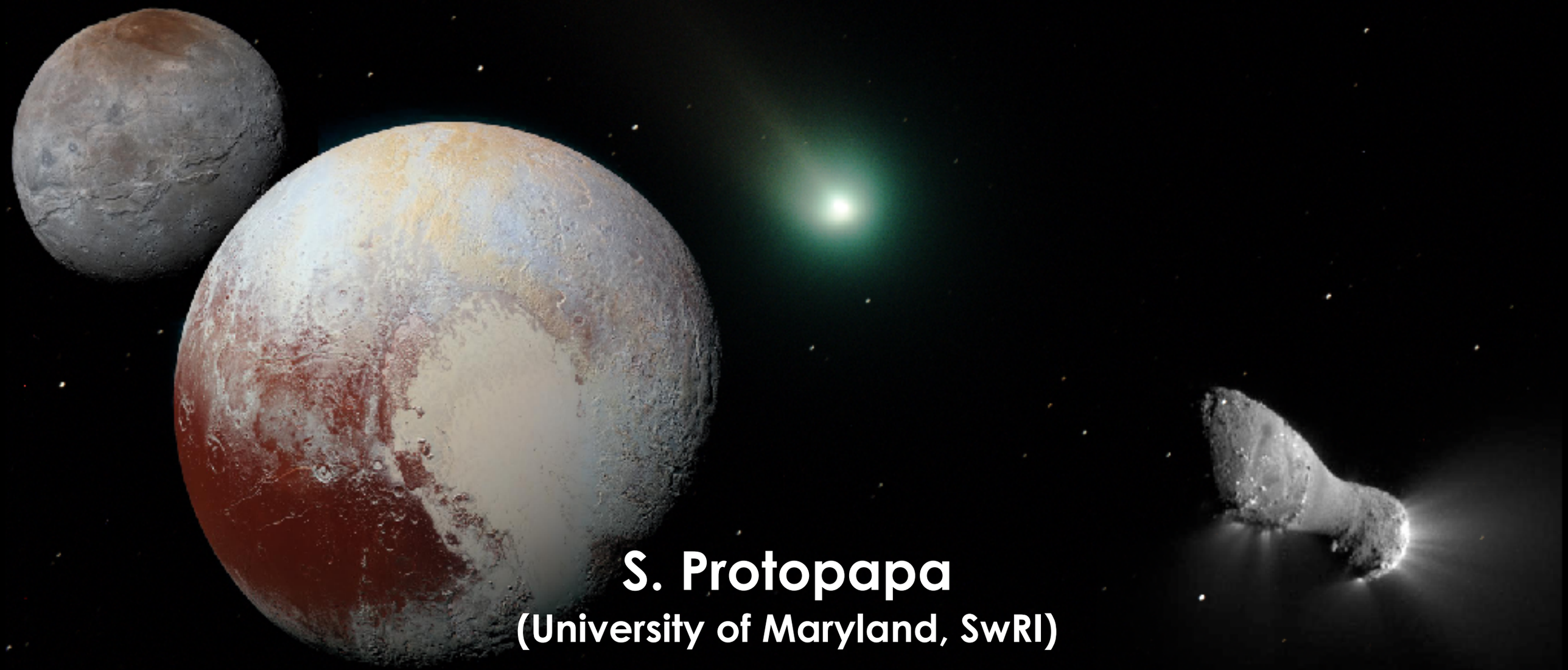
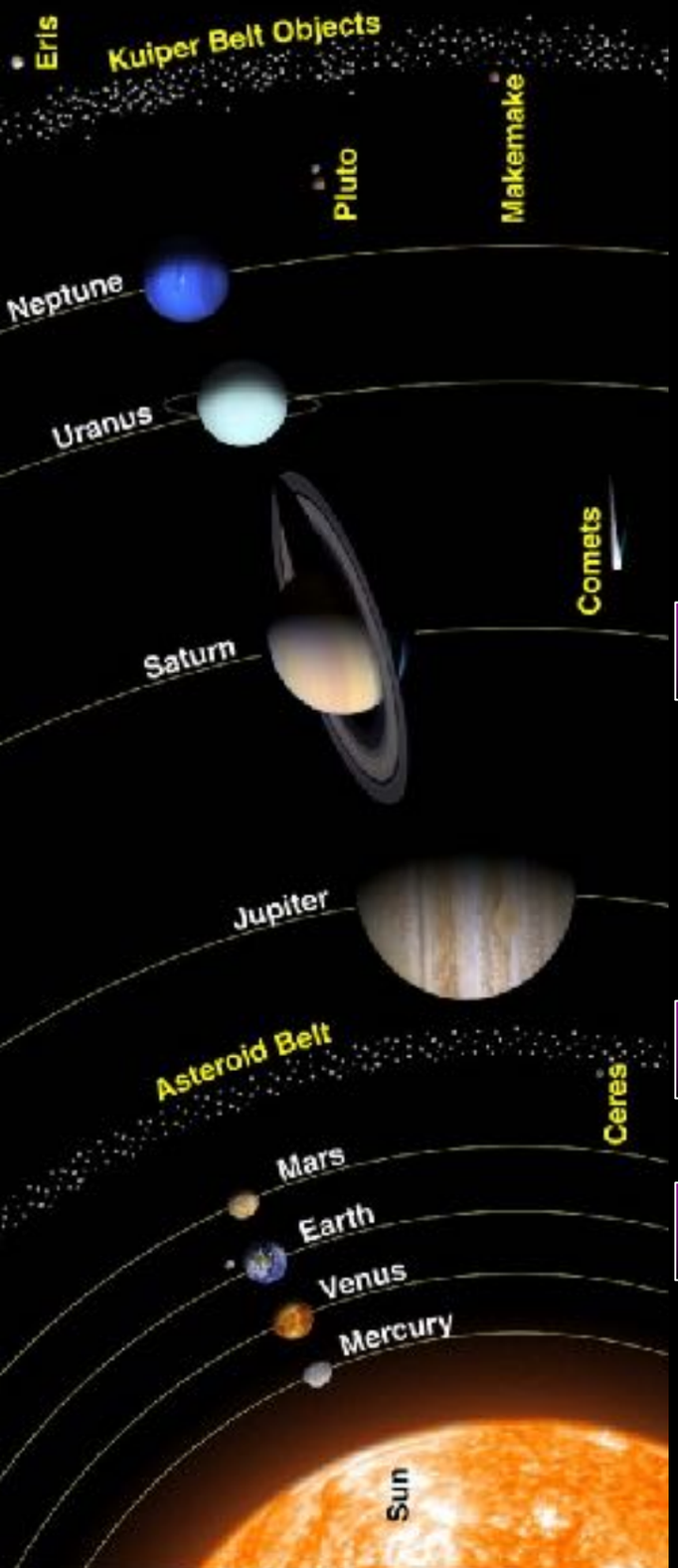
Composition of icy bodies in the outer solar system through the eyes of IRTF: current and future



S. Protopapa
(University of Maryland, SwRI)

Scientific interests



Objects of Study

Trans-Neptunian objects (TNOs)

Comets

Asteroids

The Moon

Goal

formation and evolution of the solar system

Methodology

COMPOSITION ANALYSIS

- ground and space based observations
- modeling efforts
- laboratory studies

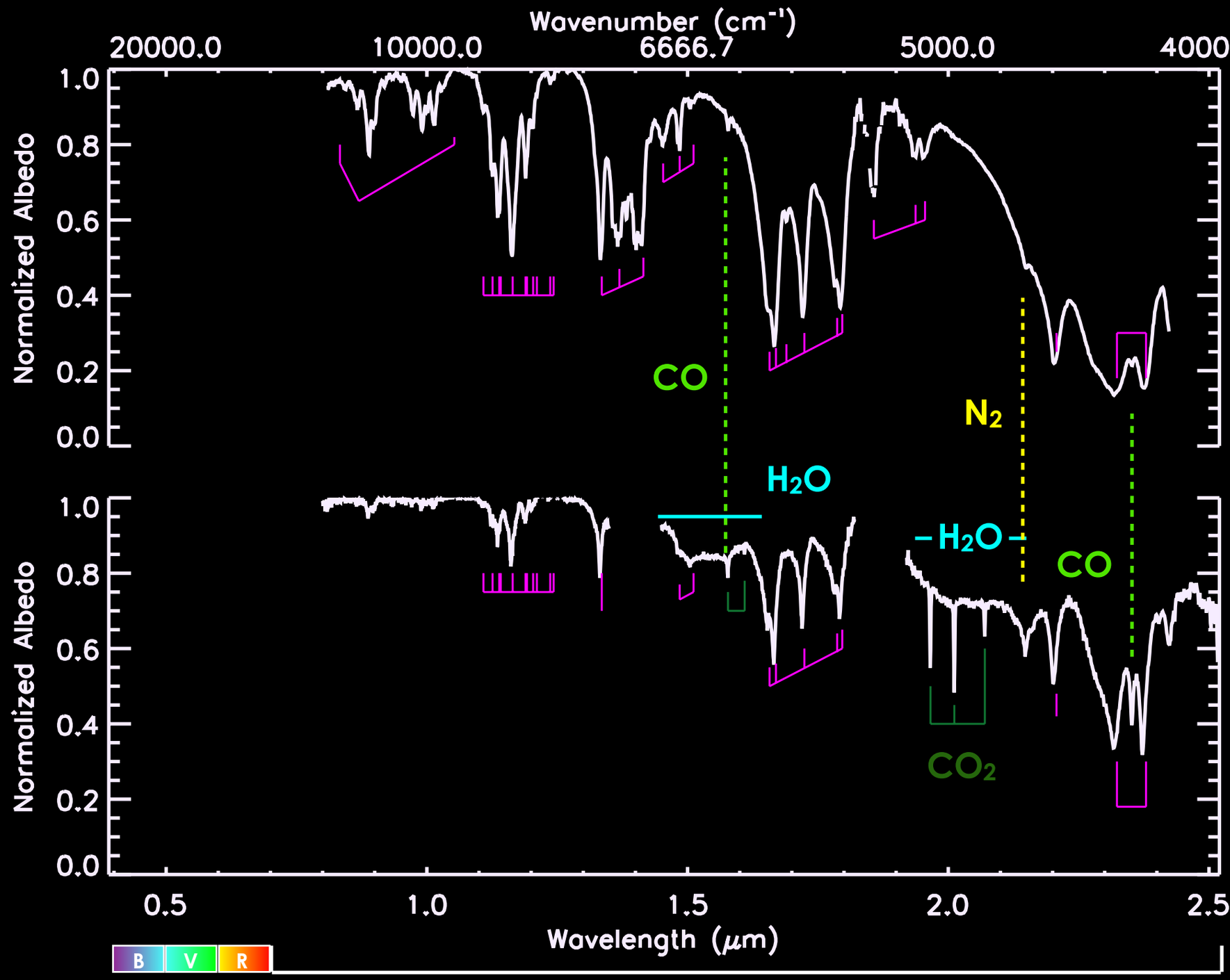
Future directions



- low resolution visible spectrometer (0.3-0.7 μm)
- Adaptive optics
- Implement Spextool to reduce data taken with the 60”-slit
- IRTF facility in the south
- low resolution prism extending up to 4.2 μm (R~200)

Pluto versus Triton





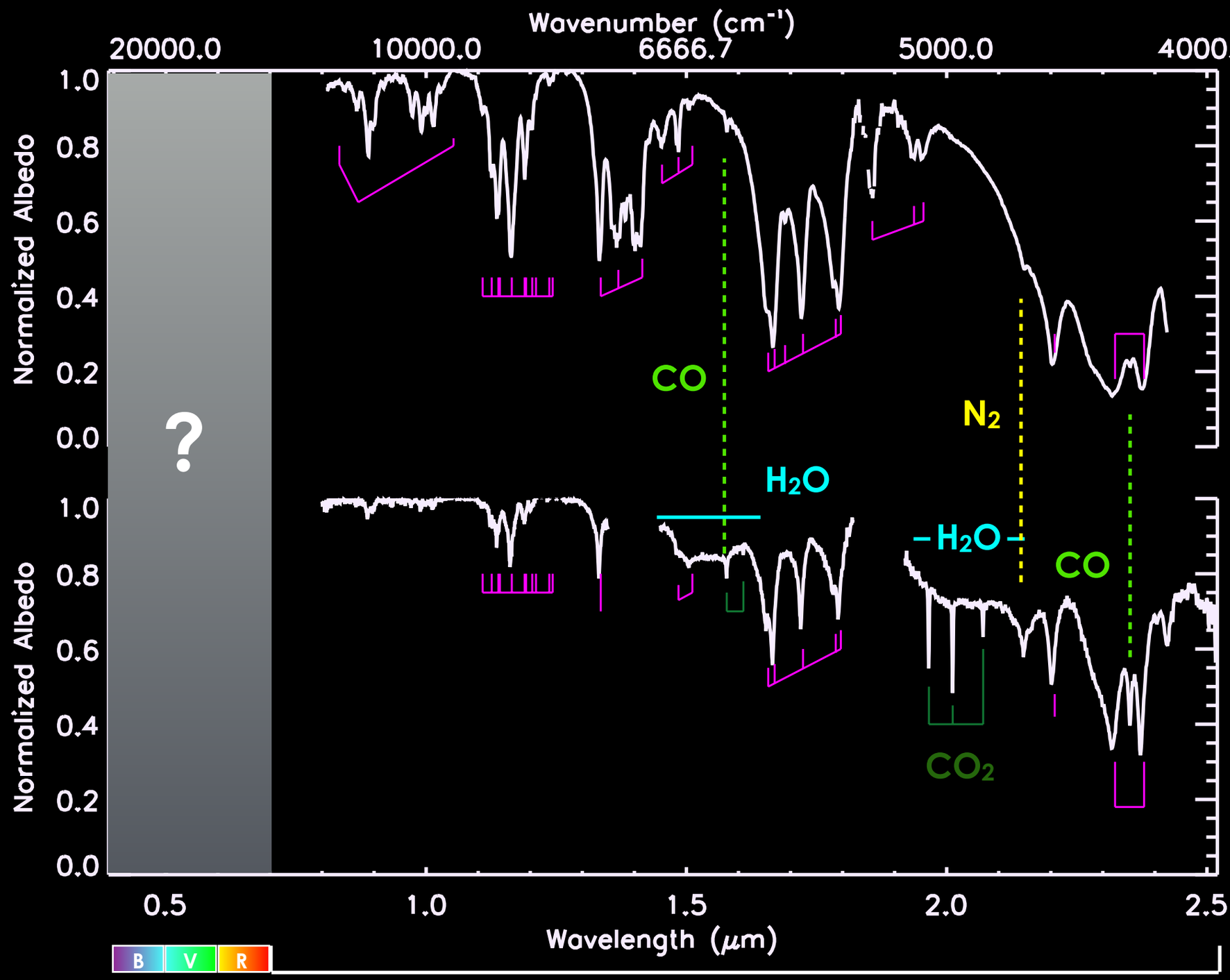
Grundy et al. 2013
IRTF/SpeX Pluto
short cross-dispersed mode

Grundy et al. 2010
IRTF/SpeX Triton

IRTF/SpeX PRISM 0.7-2.52 μm

Pluto versus Triton





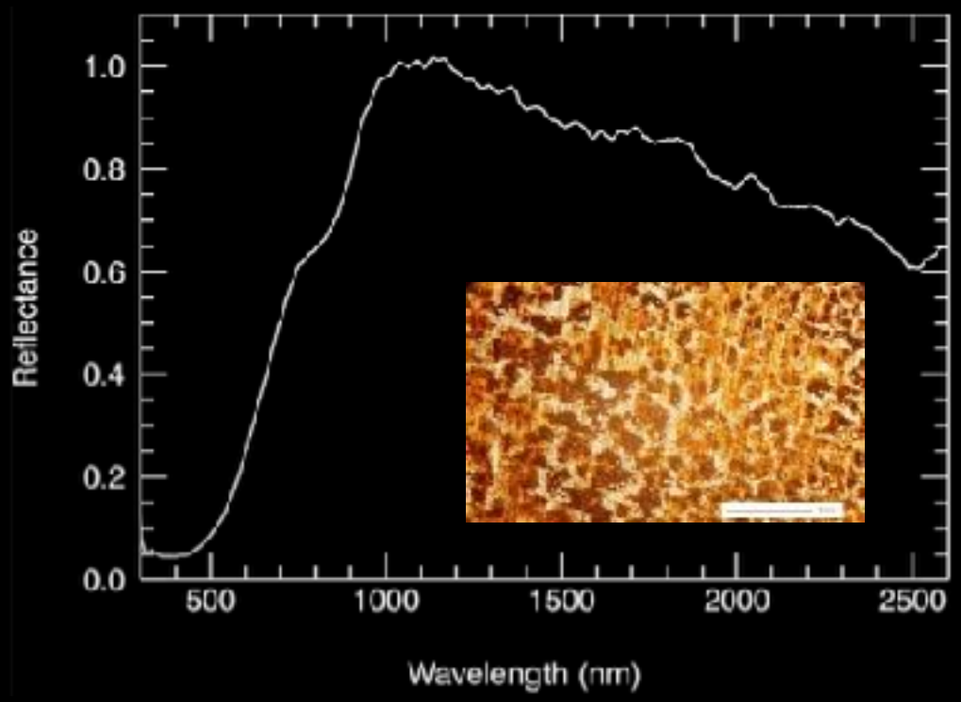
Grundy et al. 2013
IRTF/SpeX Pluto

Grundy et al. 2010
IRTF/SpeX Triton

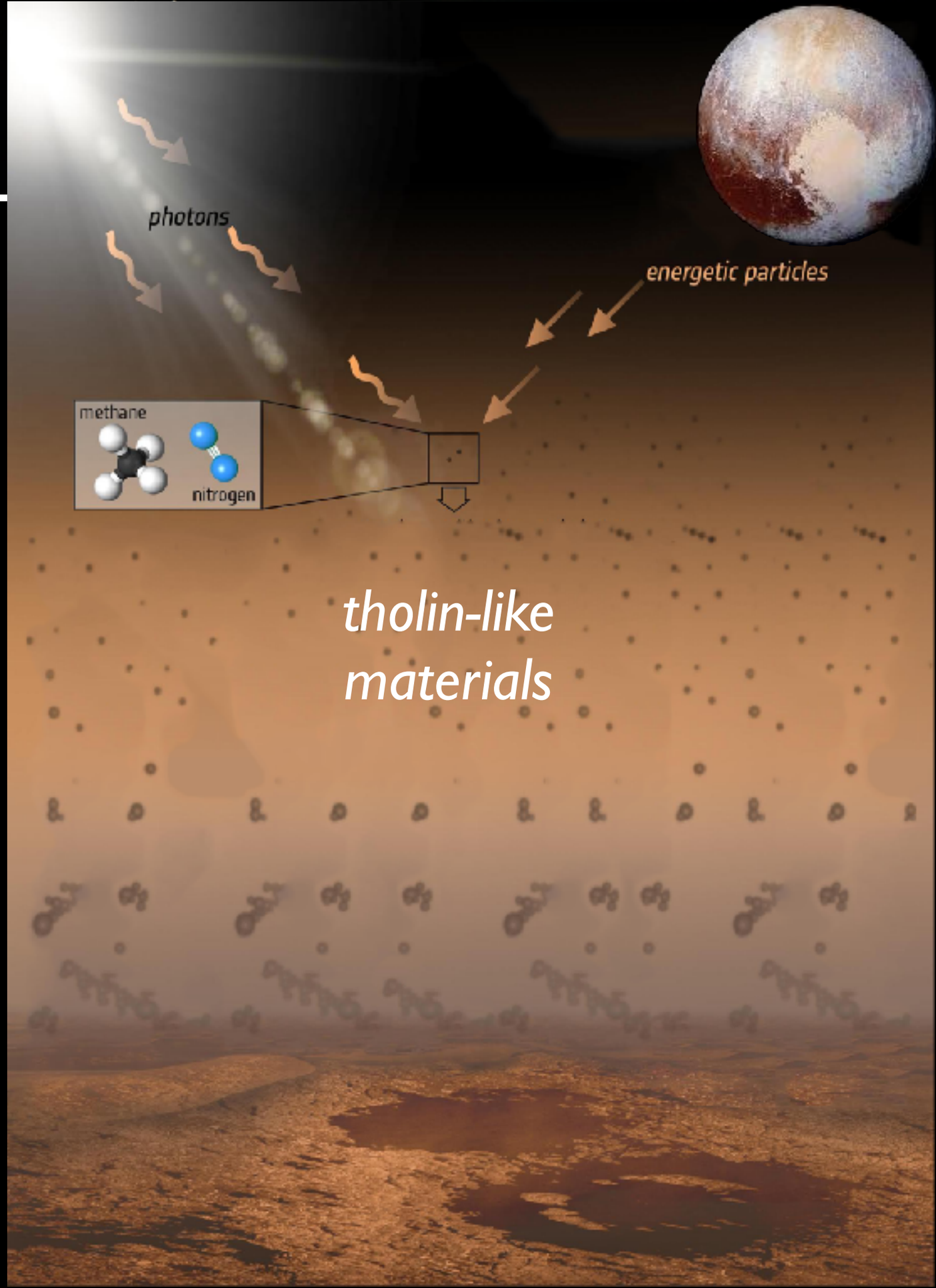
VIS IRTF/SpeX PRISM 0.7-2.52 μm

Tholin-like material

(Matarese et al. 2015, Cruikshank et al. 2016) laboratory data

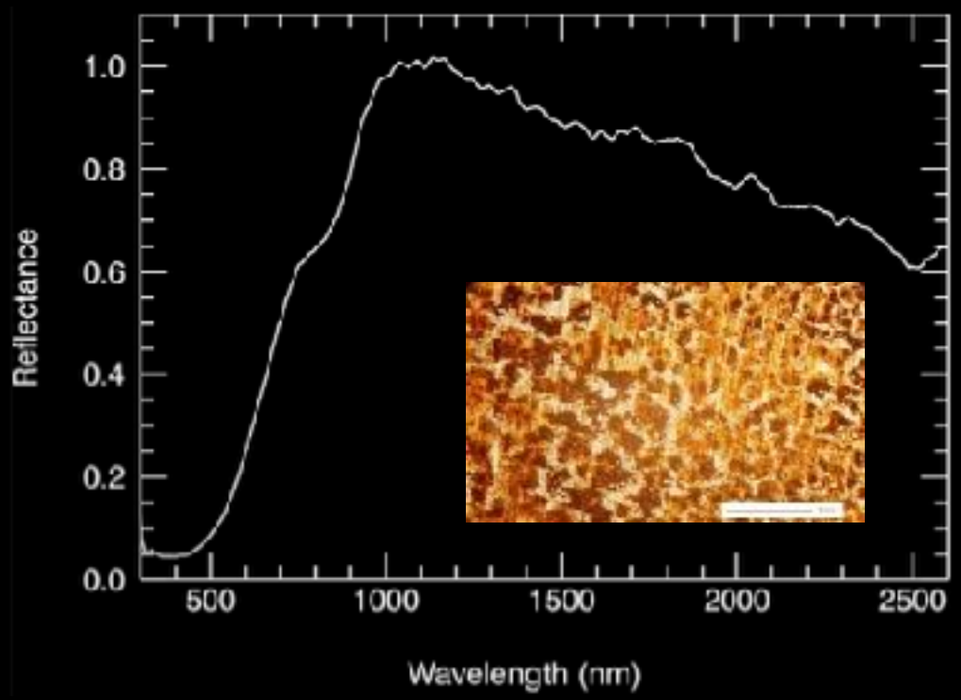


Reflectance spectrum of Pluto's ice tholin obtained in the laboratory. The steep rise in reflectance in the range from~400nm to 1000nm demonstrates the red-orange color of the material

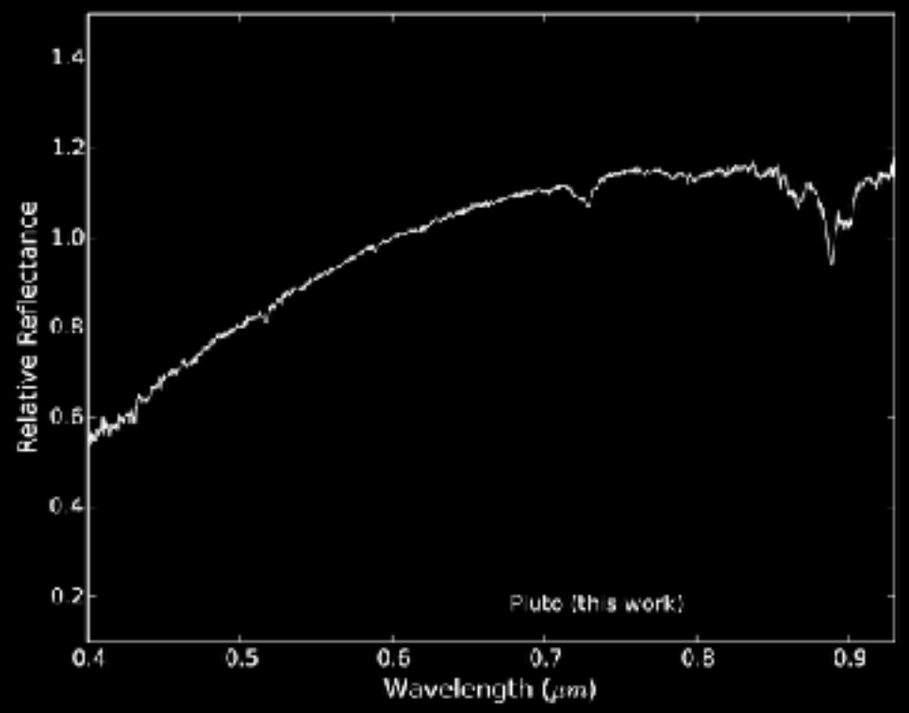


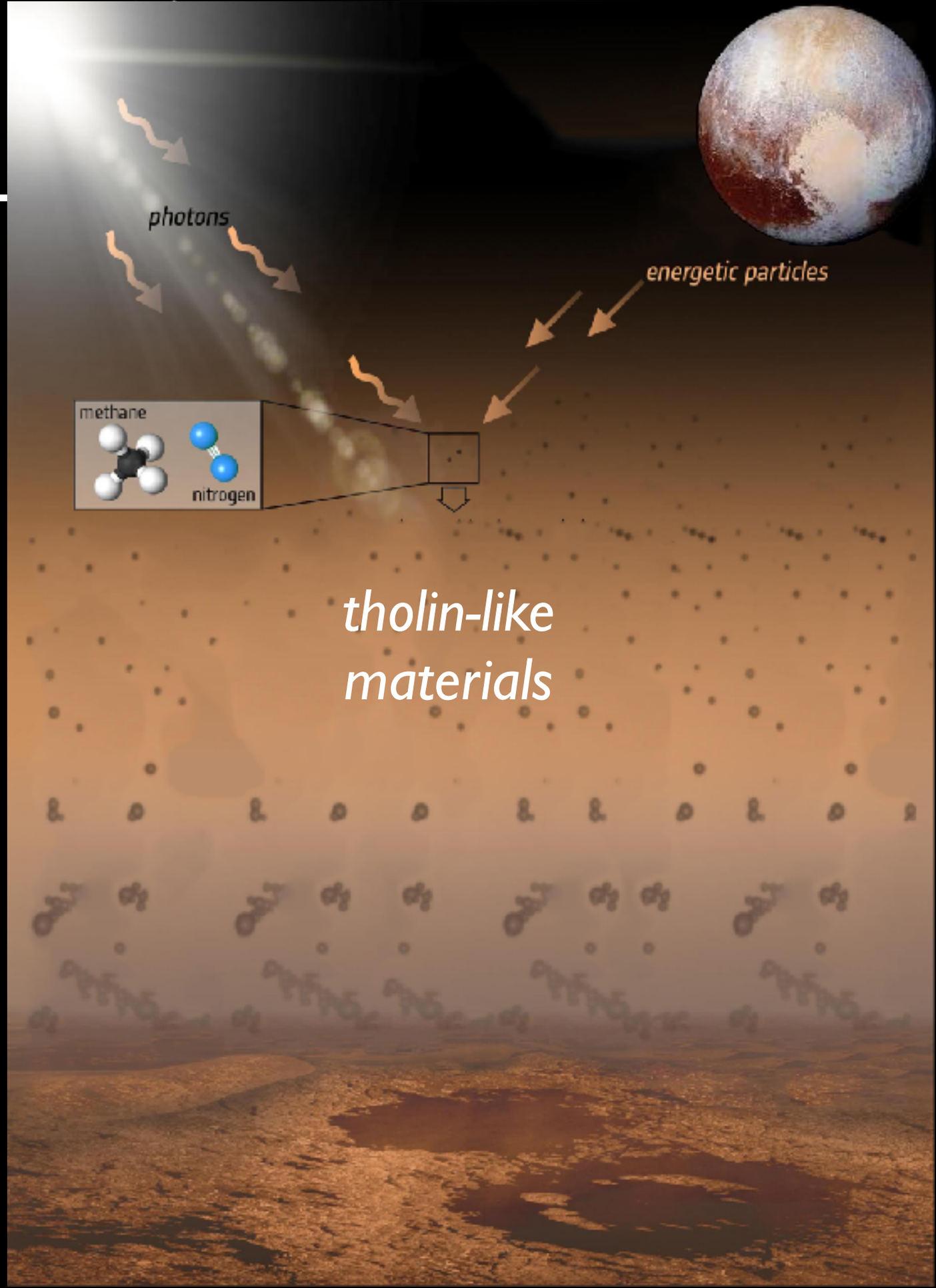
Tholin-like material

(Matarese et al. 2015, Cruikshank et al. 2016) laboratory data



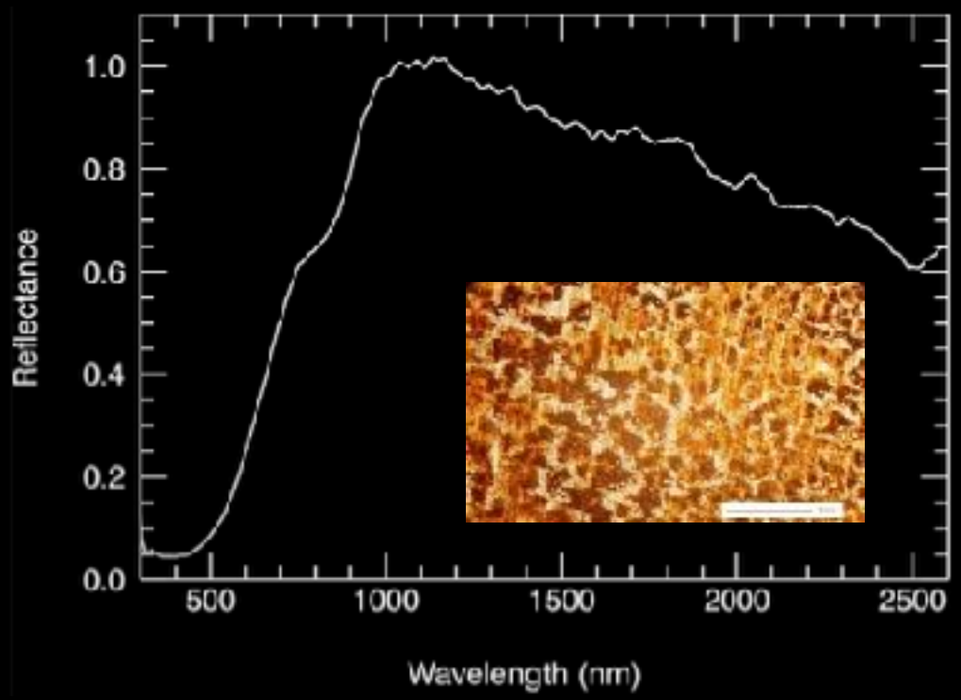
Lorenzi et al. 2016 *ground-based data*





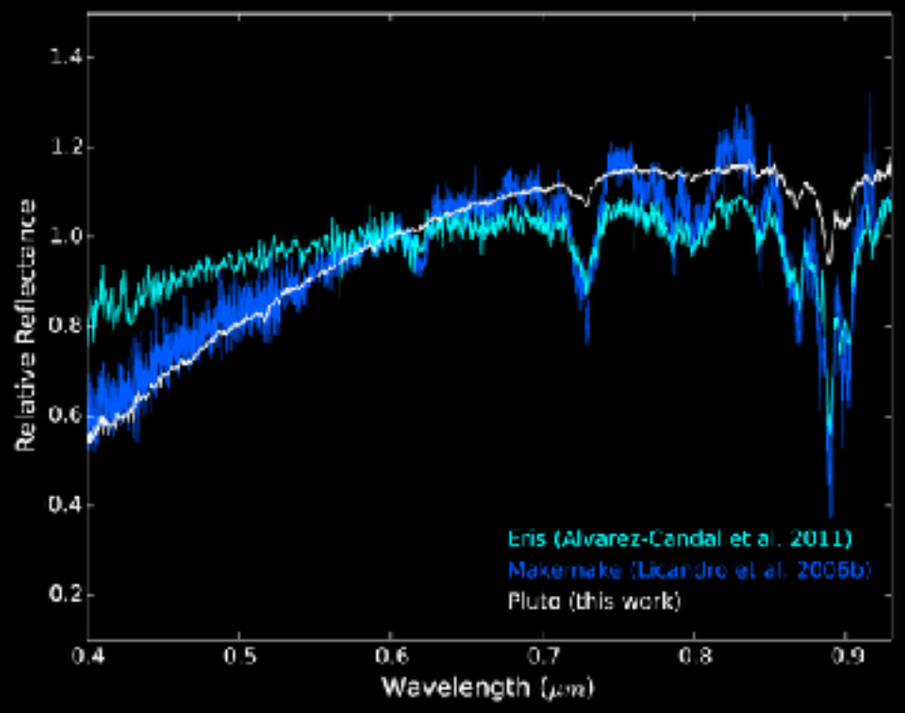
Tholin-like material

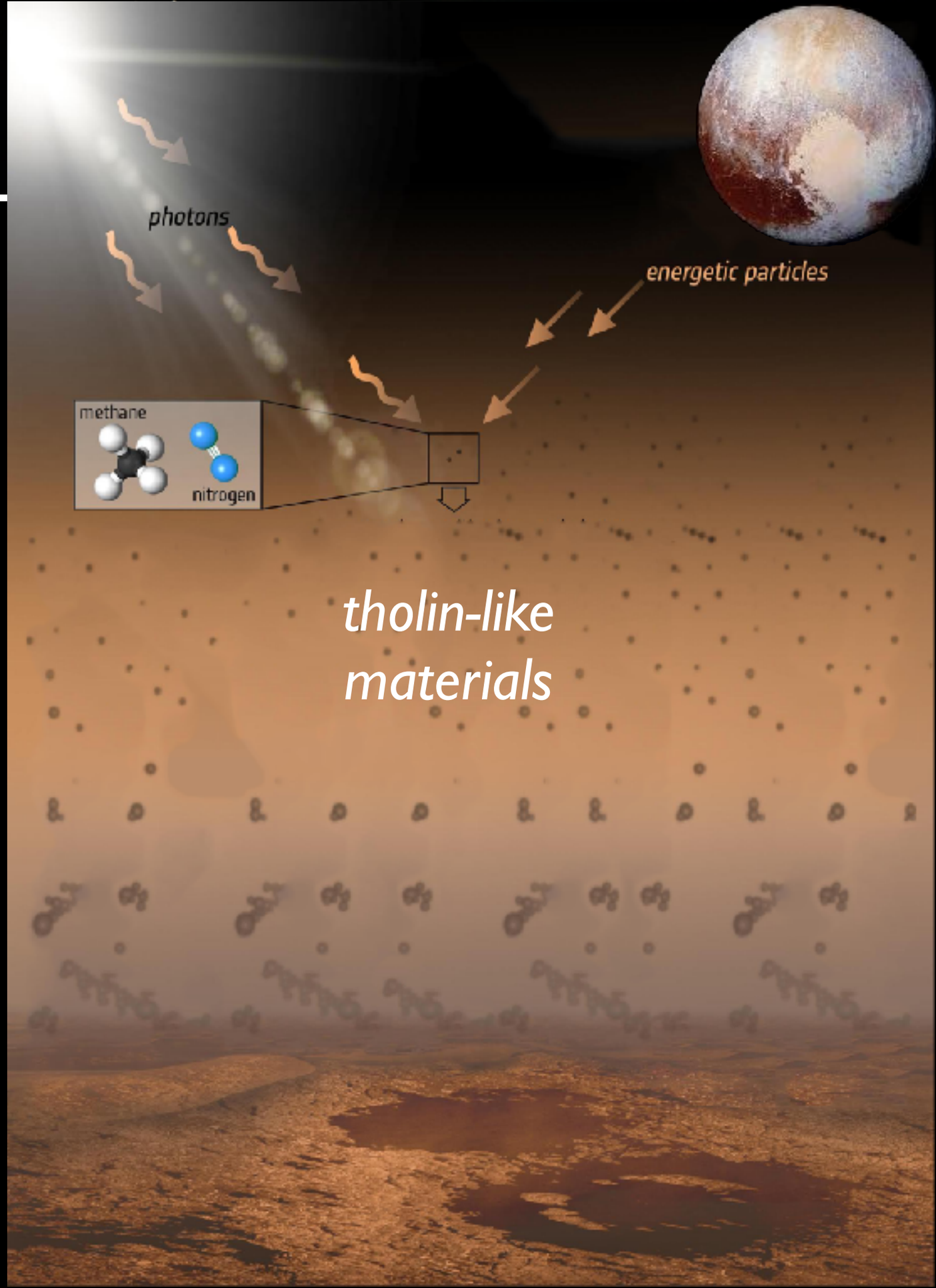
(Matarese et al. 2015, Cruikshank et al. 2016) laboratory data



Lorenzi et al. 2016

ground-based data

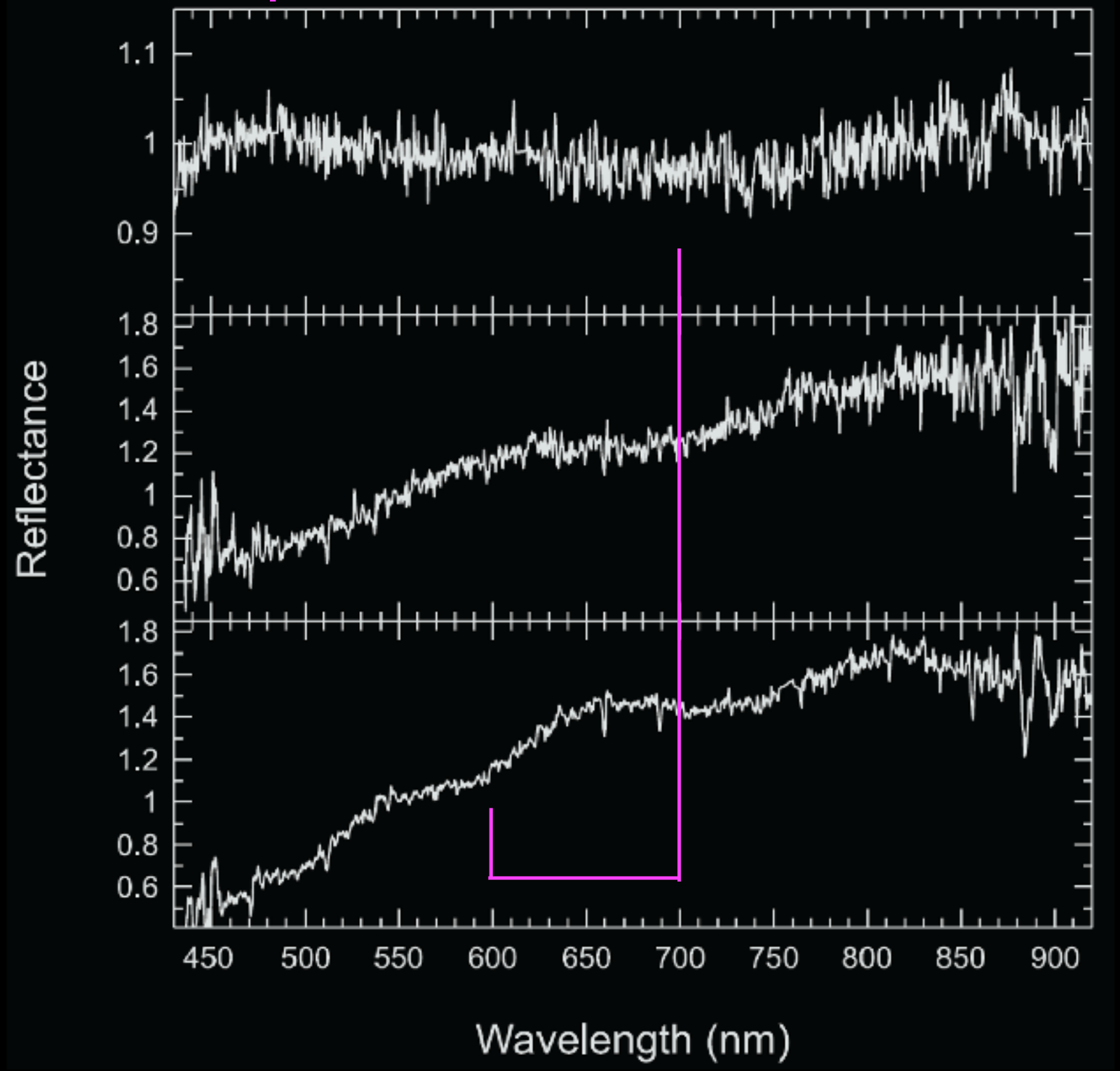




Why not photometry with MORIS?



aqueous alteration bands in the visible



2003 AZ_{84}, (Fornasier et al. 2004)

47932 GN_{171} (Lazzarin et al. 2003)

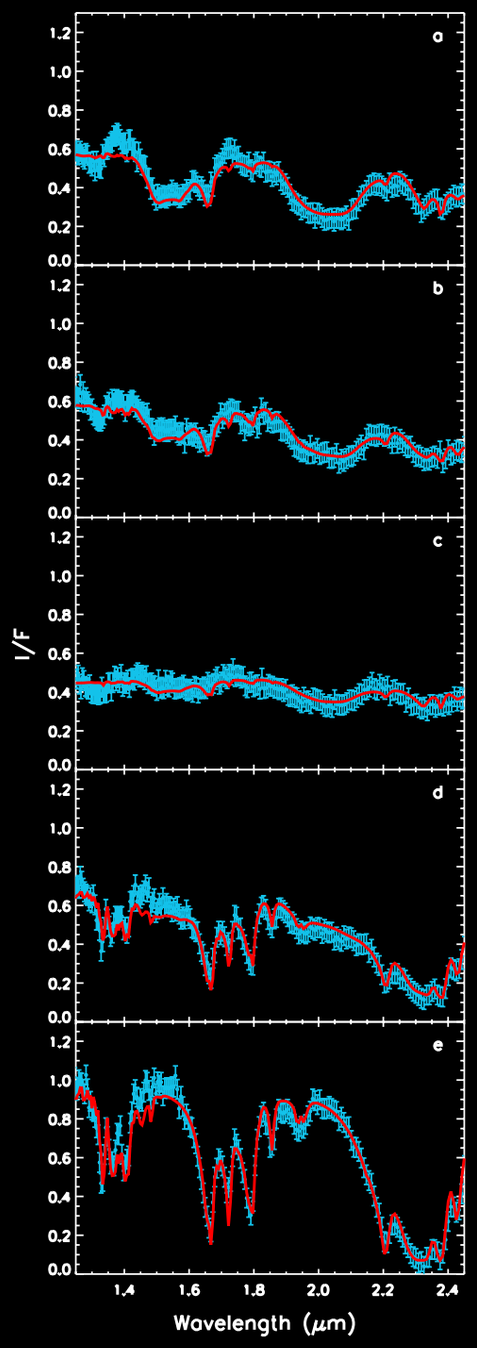
38628 Huya (Lazzarin et al. 2003)

Pluto/wide surface heterogeneity

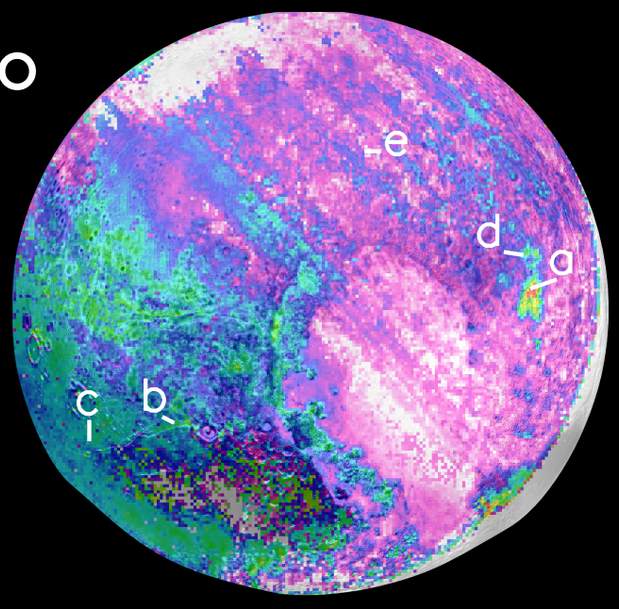


NON-VOLATILES

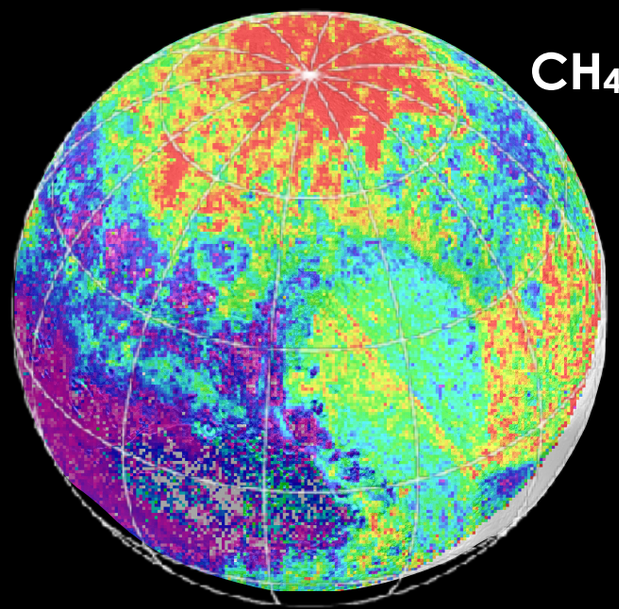
VOLATILES



H_2O



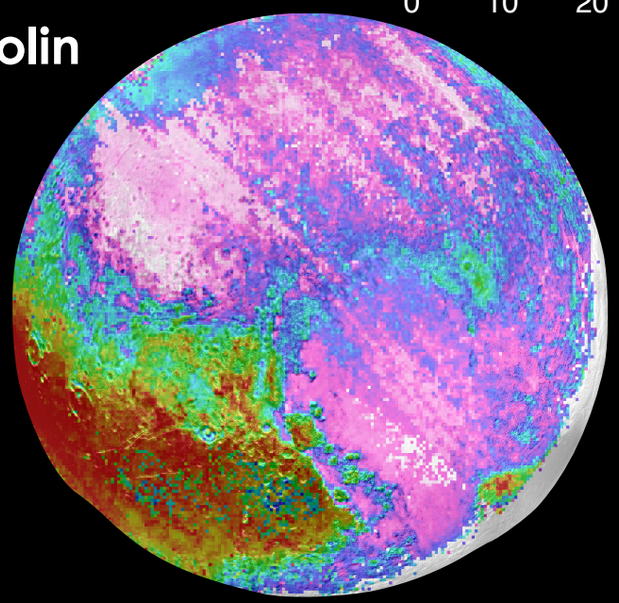
$CH_4:N_2$



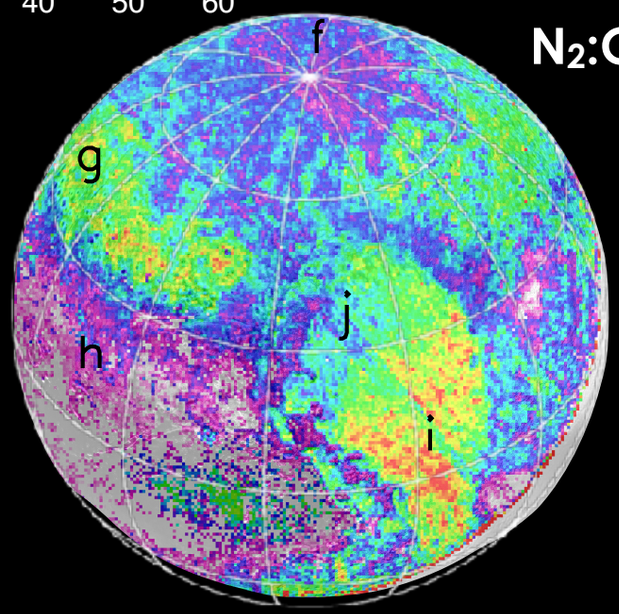
F %

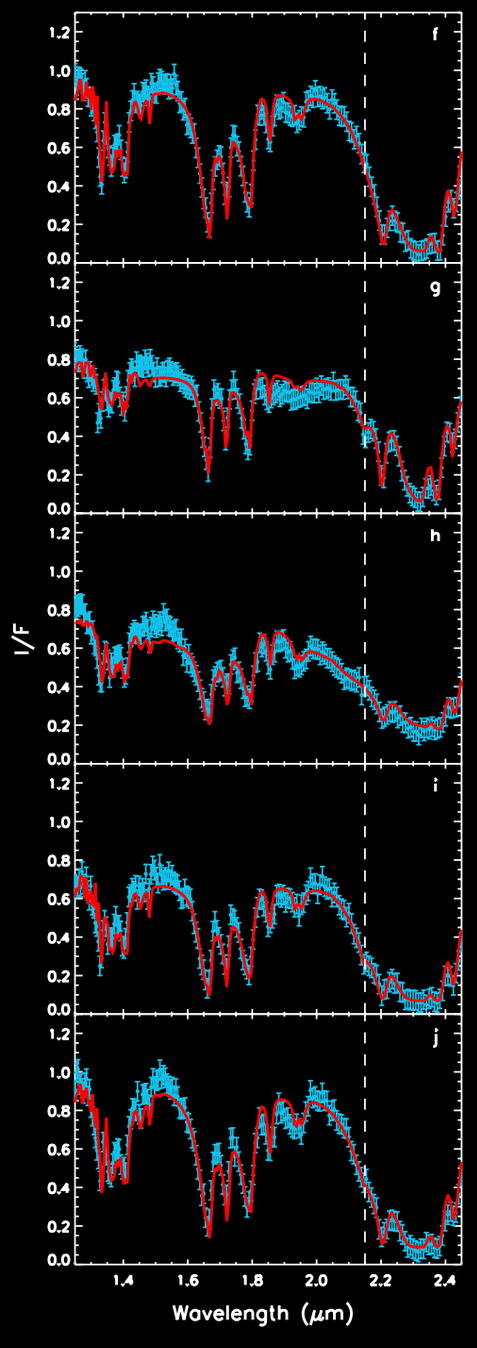


Tholin



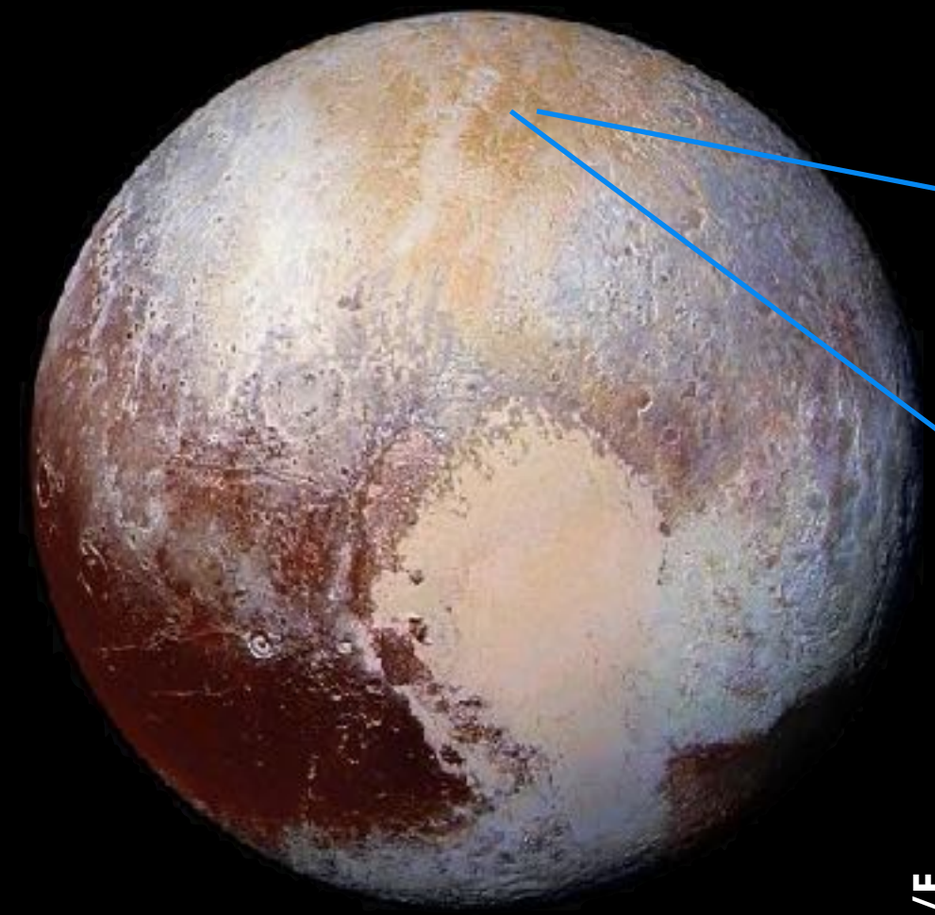
$N_2:CH_4$





Protopapa et al., 2017

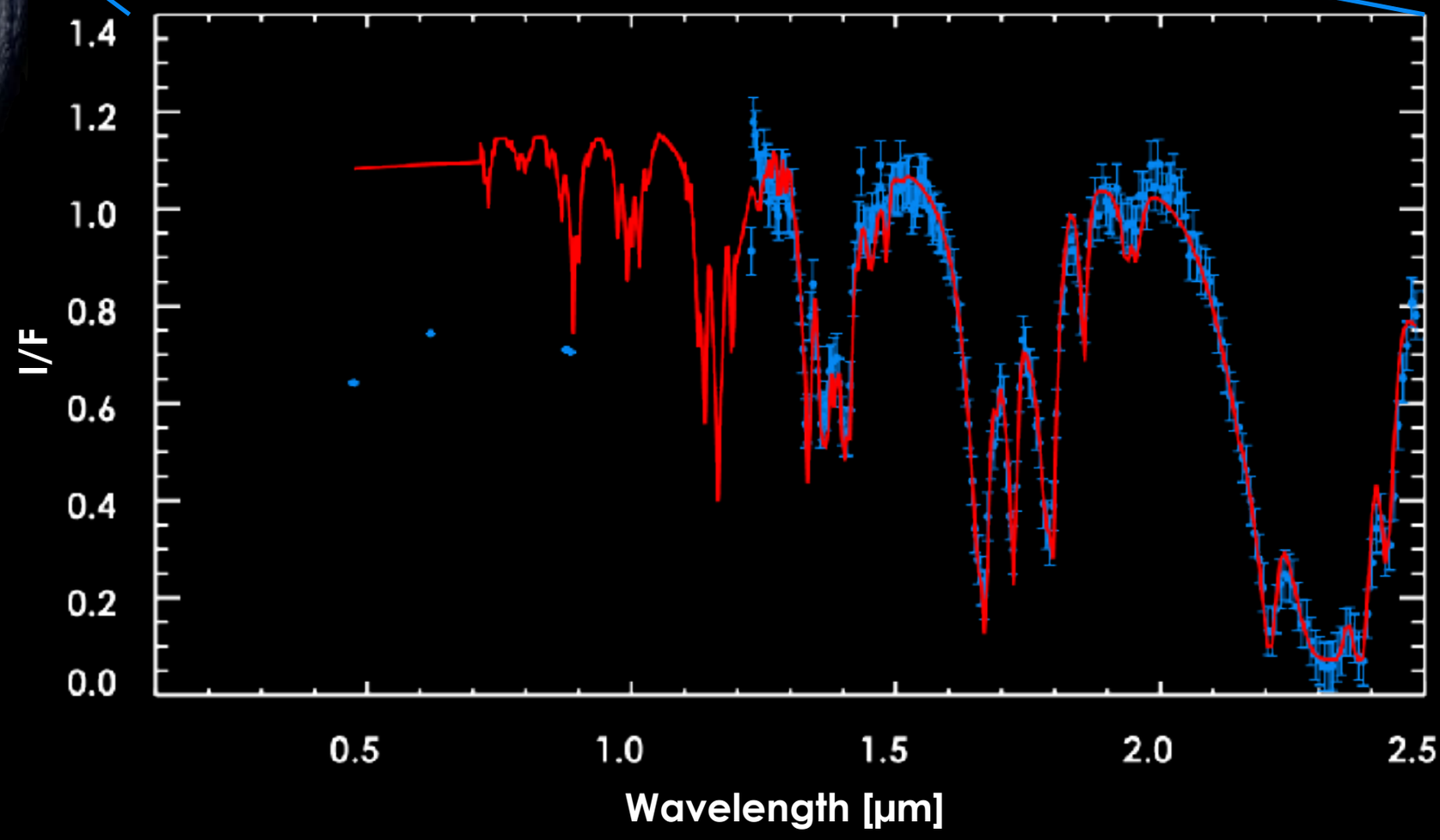
Simultaneous VIS+NIR observations



Stern et al. 2015
Credits: NASA/JHUAPL/SwRI

New Horizons data

modeling with CH_4:N_2, N_2:CH_4, H_2O
no tholins

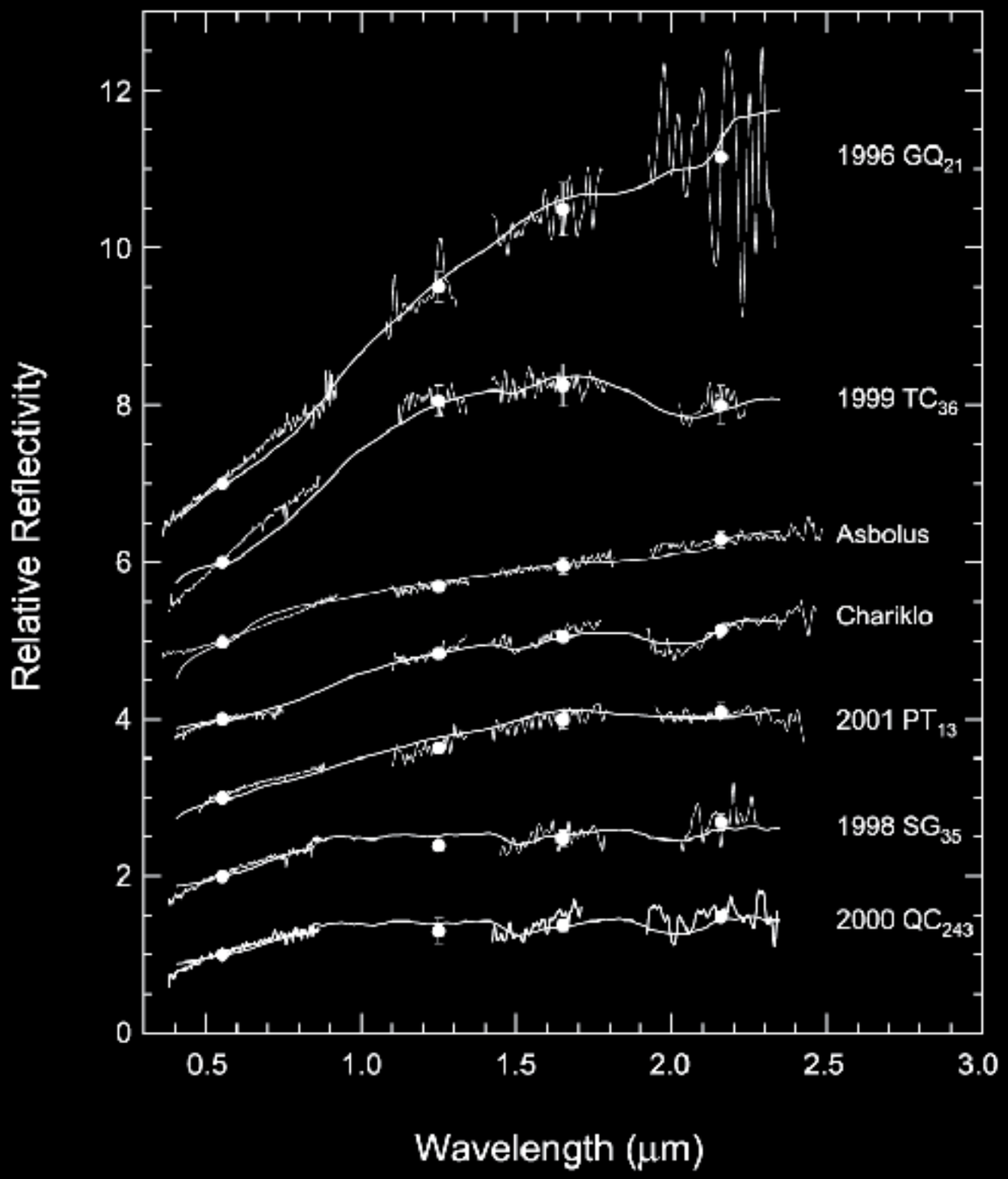


Protopapa et al. in prep

Simultaneous VIS+NIR observations



Barucci et al. 2005



V + NIR spectra of two TNOs and five Centaurs

ESO-VLT

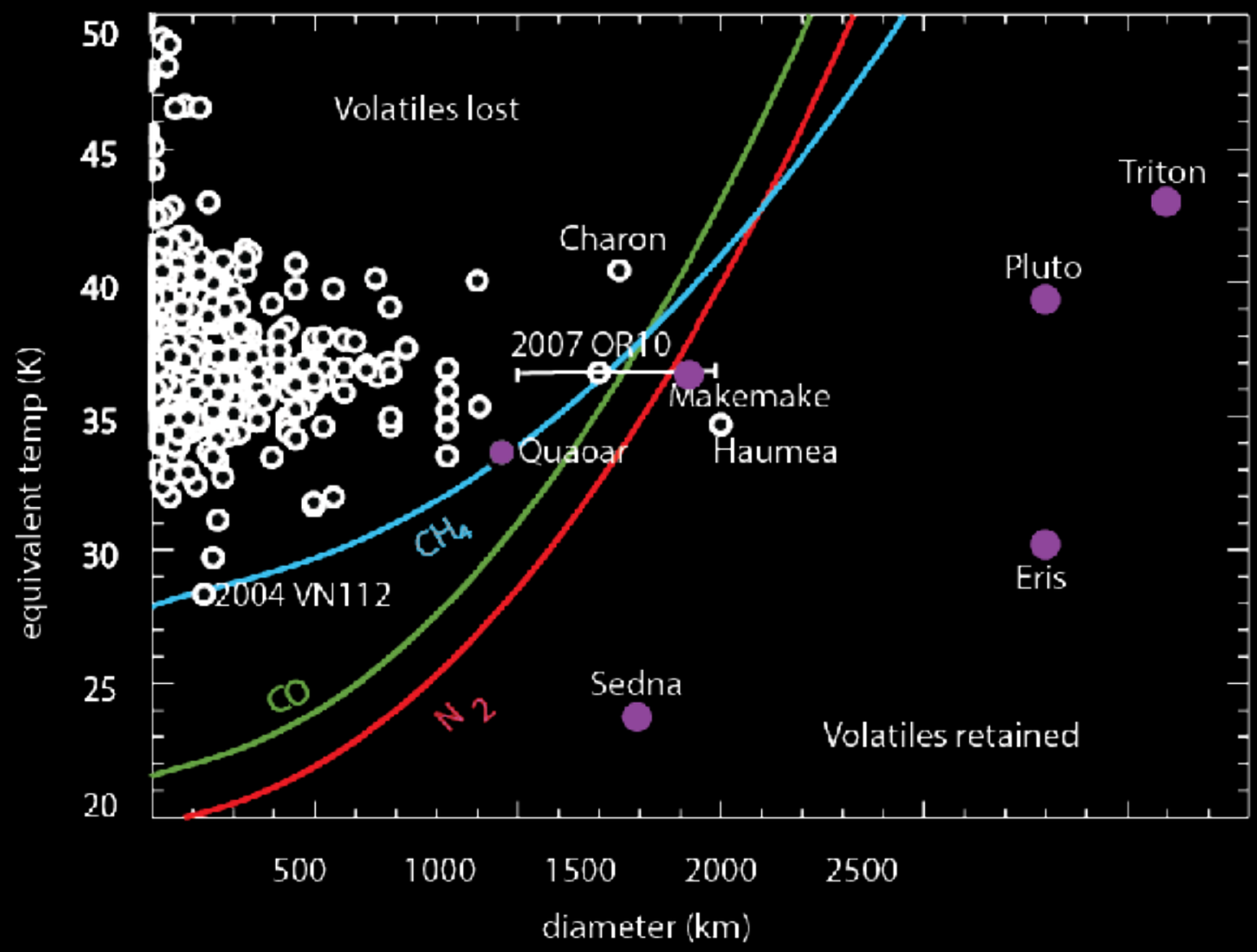
VIS —> FORS 1/Unit Telescope 2 (Kueyen)

NIR —> ISAAC/Unit Telescope 1 (Antu)

Volatile retention and loss in the Kuiper belt

small, volatile-poor but extremely primitive planetesimals

adapted from **Brown, Burgasser, Fraser 2011**

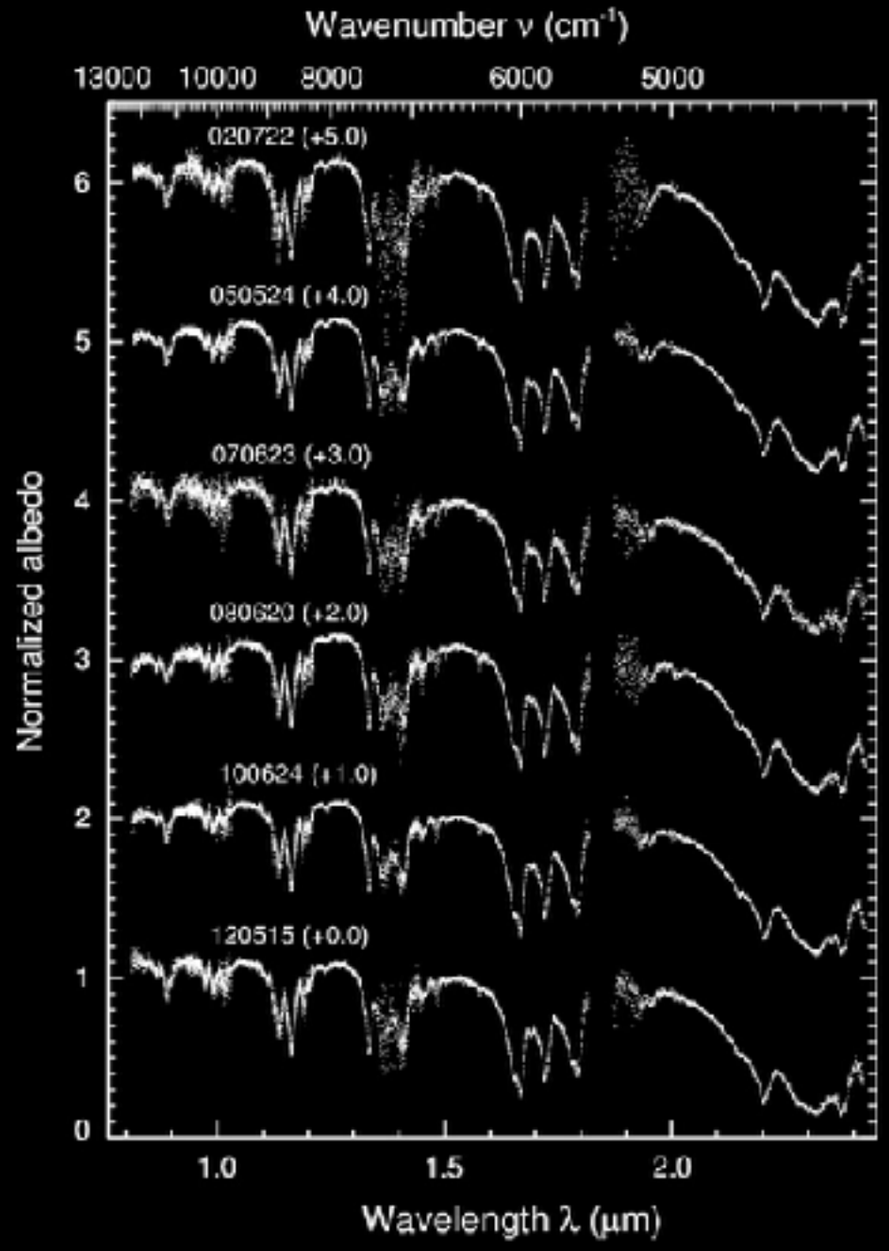


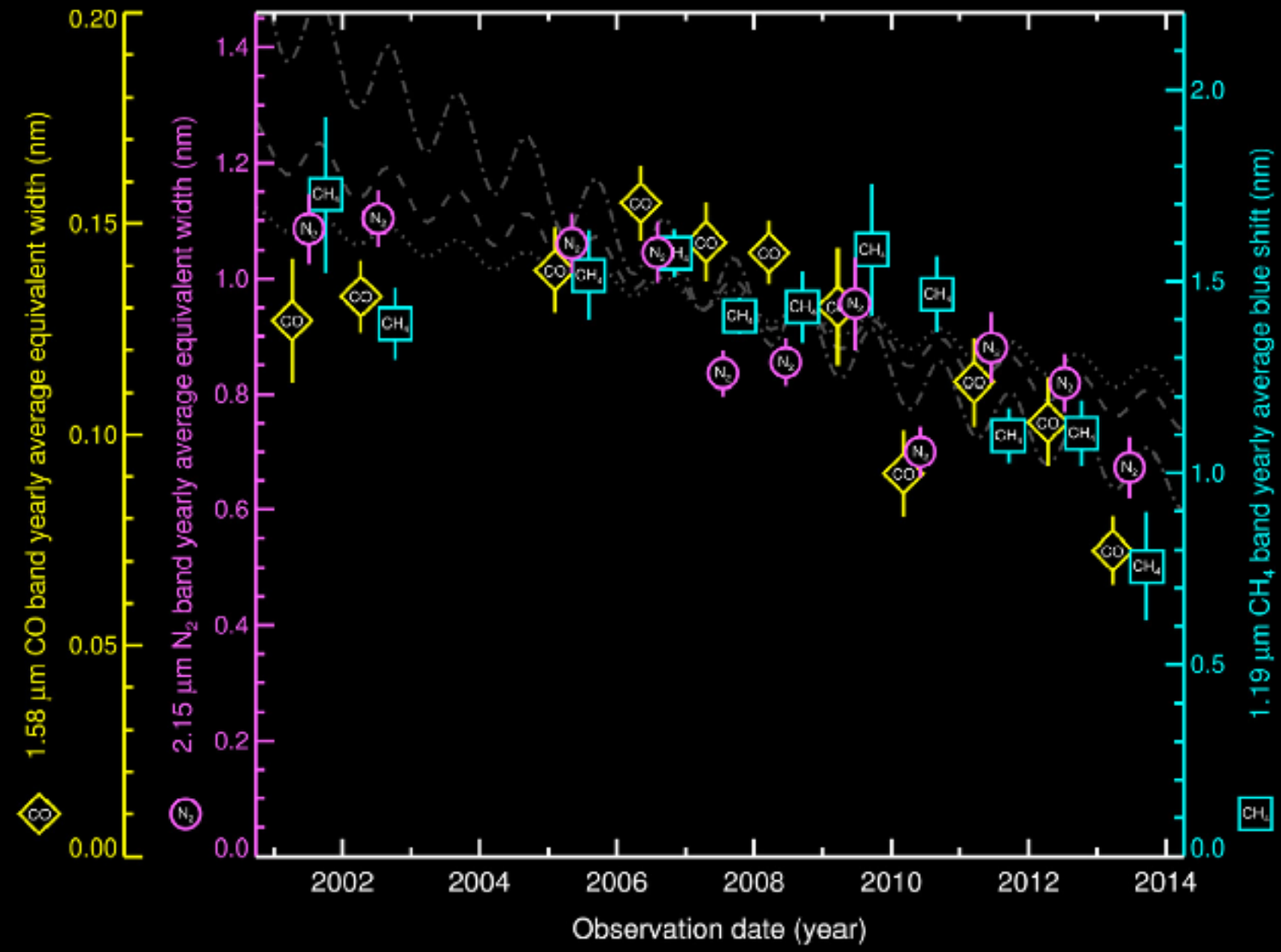
IRTF program: Spectra of the Intermediate-sized Kuiper Belt Objects / B. Holler, L. Young, S. Protopapa

geologically active, atmosphere-bearing, volatile-dominated dwarf planets

Temporal changes:
IRTF/SpeX critical for New Horizons data interpretation

Grundy et al. 2013, 2014





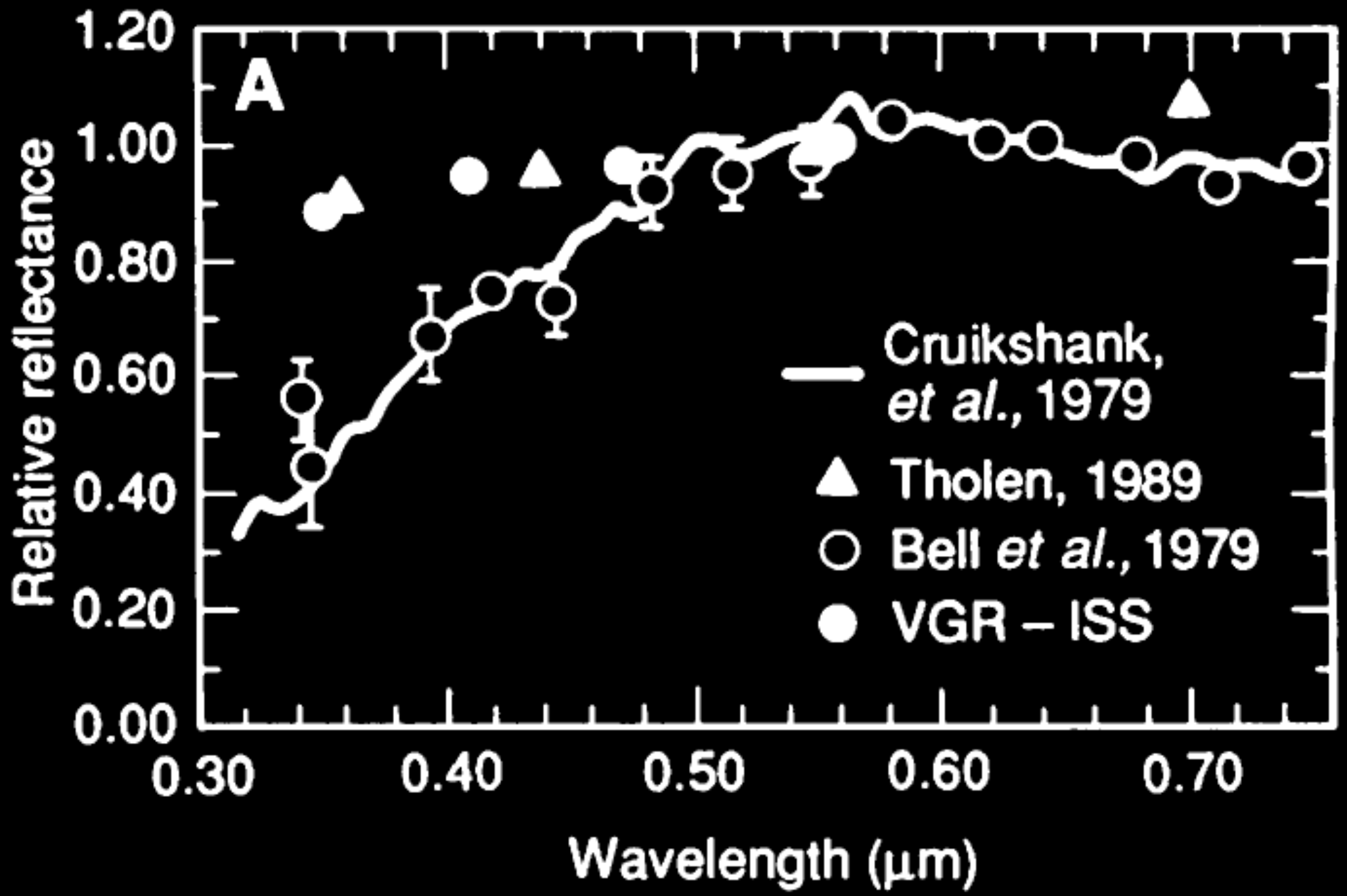
- IRTF/SpeX data of Pluto
- Observed on 70+ usable nights from 2000 - 2013
- Strategy: rotationally resolved spectra spanned over time

Similar program for Triton led by L. Young

Temporal changes: VIS spectroscopy



Smith et al. 1989



Summary

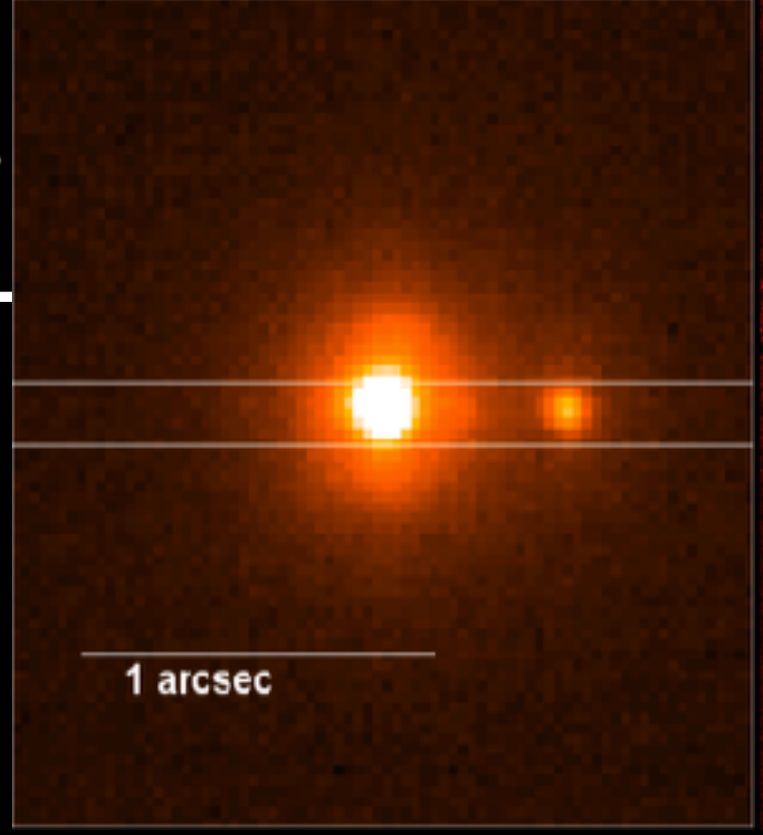


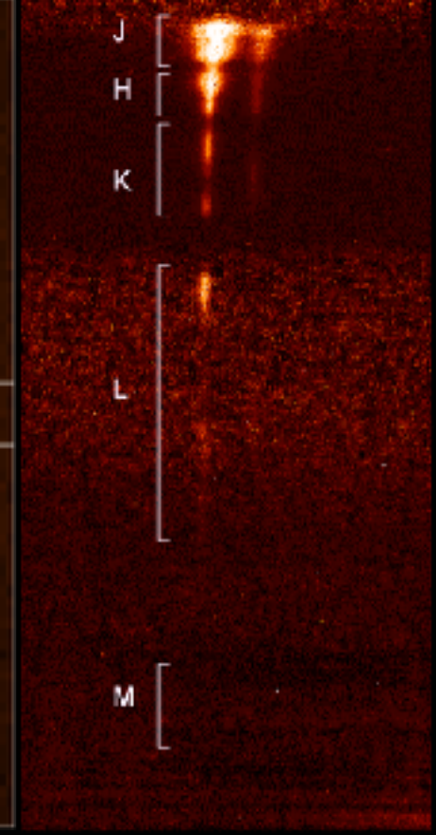
VIS spectroscopy critical to
1) characterize tholin-like material,
2) identify aqueous alteration bands,
3) correctly interpret IR measurements,
4) Investigate temporal changes

Adaptive optics

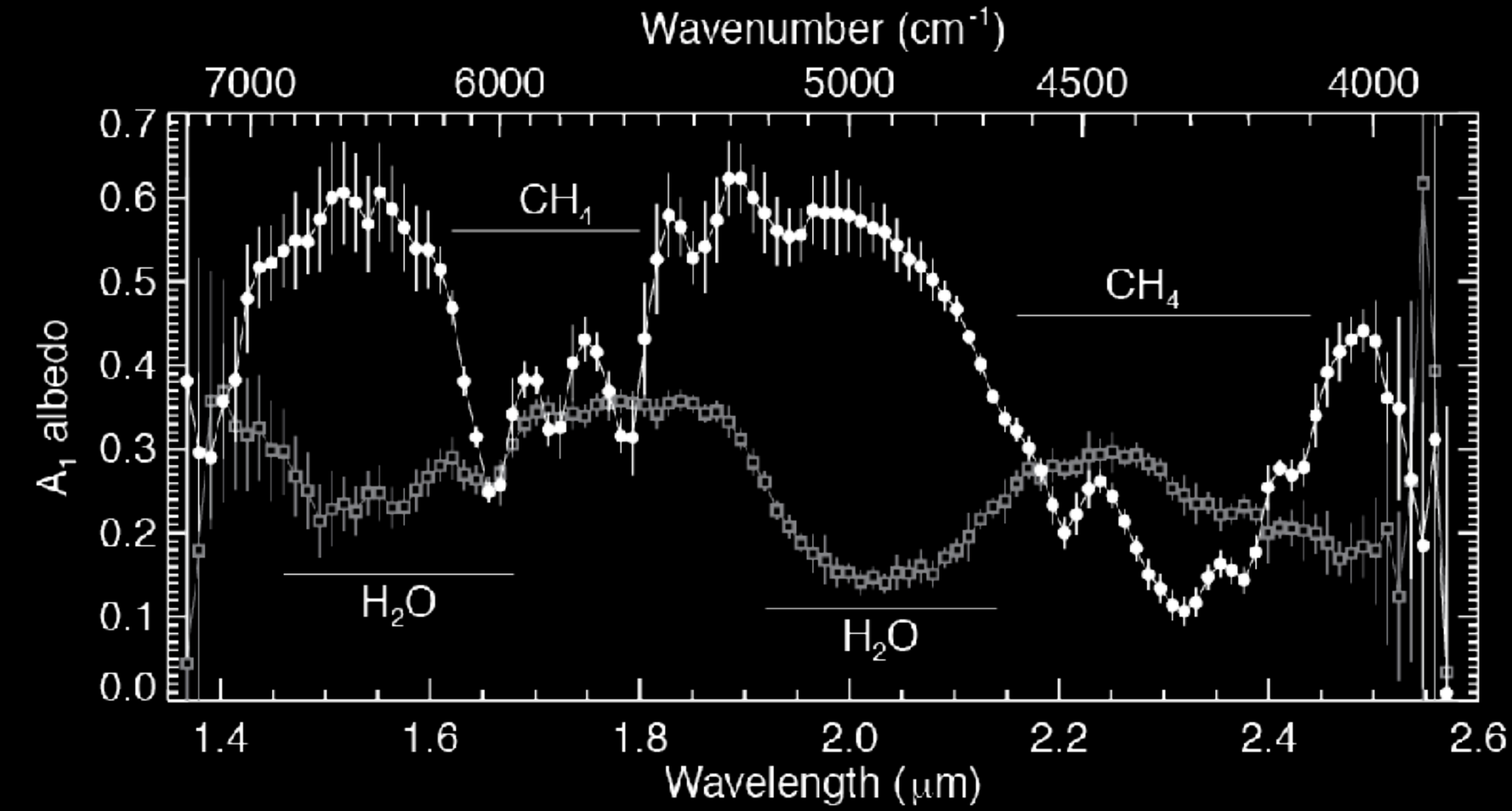
IRTF/SpeX: Pluto and Charon blended in the spectra.

<u>Problem 1</u>: the amount of light received from Charon is highly variable, depending on the separation between the two objects, seeing conditions, slit width, and the orientation of the slit relative to the Pluto-Charon position angle.





NACO/VLT
Protopapa et al. 2008



HST/NICMOS
Grundy & Buie, 2002

Adaptive optics



IRTF/SpeX: Pluto and Charon blended in the spectra.

<u>Problem 1</u>: the amount of light received from Charon is highly variable, depending on the separation between the two objects, seeing conditions, slit width, and the orientation of the slit relative to the Pluto-Charon position angle.

<u>Problem 2</u>: Charon surface composition might not be constant over time (Grundy et al. 2016)

<u>Problem 3</u>: Lost opportunities: e.g., In July 2018 the Earth transited the disk of the Sun as seen from Pluto and Charon, presenting the rare opportunity to make observations of these outer solar system objects at the smallest possible phase angle (<0.01°). The last time Pluto and Charon were visible at such small phase angles was 1931, the year after Pluto was discovered and long before astronomers understood the rich information contained within solar phase curves. Owing to the eccentricity of Pluto's orbit, Pluto and Charon will not be visible at phase angles this small again for another 161 years.



Stern et al. 2015

Credits: NASA/JHUAPL/SwRI

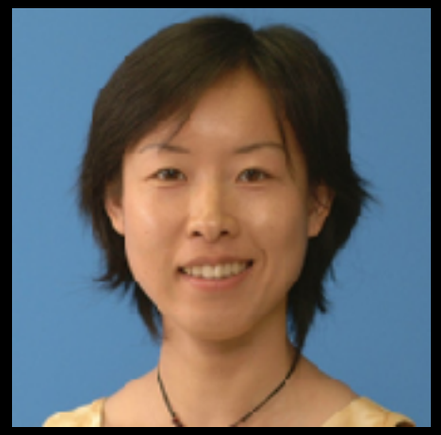
IRTF/SpeX survey of water-ice grain halos

NASA Solar System Observations Program (PI: Protopapa)

~ 30 comets



Kelley (UMD)



Yang (ESO, Chile)



Woodward (MN Institute of Astrophysics)

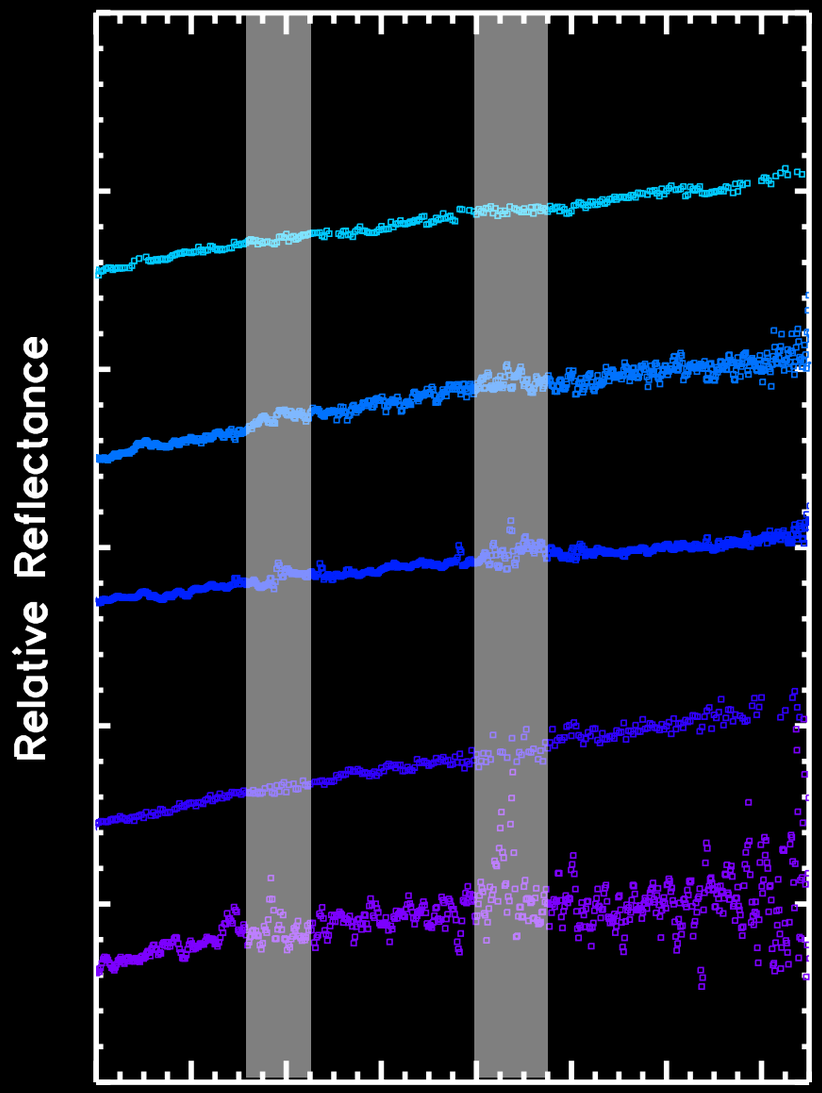
Target	Telescope/Instrument	Semester	Date	Class	r_h [a]	Δ [b]	PI	Observers
C/2013 A1 (Siding Spring)	IRTF/SpeX	2013B016	2014-01-26	OCC	3.7	3.7	Jones	Kelley/Woodward/Protopapa
C/2010 S1 (LINEAR)	IRTF/SpeX	2014B024	2014-08-12	OCC	6.7	5.9	Keane	Yang/Protopapa
117P/Helin-Roman-Alu 1	IRTF/SpeX	2014B024	2014-08-12	JFC	3.1	2.1	Keane	Yang/Protopapa
	IRTF/SpeX	2014B024	2014-08-13		3.1	2.1	Keane	Kelley/Protopapa
Catalina (C/2013 US10)	IRTF/SpeX	2014B024	2014-08-12	OCC	5.8	5.0	Keane	Yang/Protopapa
	IRTF/SpeX	2014B024	2014-08-13		5.8	5.0	Keane	Protopapa/Kelley
	IRTF/SpeX	2014B008	2014-11-08	.	5.0	4.7	Yang	Yang
	IRTF/SpeX	2015B081	2015-12-29		1.1	1.0	Protopapa	Protopapa/Kelley
	IRTF/SpeX	2015B008	2016-01-12		1.3	0.7	Woodward	Woodward/Kelley
	IRTF/SpeX	2016A988	2016-03-27		2.3	2.5	Yang	Yang
	IRTF/SpeX	2016B079	2016-08-12		3.9	4.4	Protopapa	Protopapa
LINEAR (C/2011 J2)	IRTF/SpeX	2014B024	2014-08-12	OCC	4.0	3.7	Keane	Yang/Protopapa
17P/Holmes	IRTF/SpeX	2014B024	2014-08-12	JFC	2.3	2.4	Keane	Yang/Protopapa
NEOWISE (C/2014 N3)	IRTF/SpeX	2014B024	2014-08-13	OCC	4.3	3.7	Keane	Kelley/Protopapa
PANSTARRS (C/2012 K1)	IRTF/SpeX	2015A076	2015-07-09	OCC	4.3	3.9	Keane	Protopapa/Kelley
	IRTF/SpeX	2015A076	2015-07-21		4.4	3.9	Keane	Protopapa/Kelley
PANSTARRS (C/2013 X1)	IRTF/SpeX	2015B081	2015-12-28	OCC	2.1	1.7	Protopapa	Protopapa/Kelley
SONEAR (C/2014 A4)	IRTF/SpeX	2015B081	2015-12-28	OCC	4.3	4.1	Protopapa	Protopapa/Kelley
230P/LINEAR	IRTF/SpeX	2015B081	2015-12-28	JFC	1.5	0.6	Protopapa	Protopapa/Kelley
	IRTF/SpeX	2016A076	2016-02-07		1.7	0.9	Protopapa	Protopapa/Kelley
81P/Wild 2	IRTF/SpeX	2015B081	2015-12-28	JFC	2.4	1.5	Protopapa	Protopapa/Kelley
	IRTF/SpeX	2016A076	2016-02-04		2.2	1.5	Protopapa	Protopapa/Kelley
Johnson (C/2015 V2)	IRTF/SpeX	2016A076	2016-02-04	OCC	5.7	5.0	Protopapa	Protopapa/Kelley
	IRTF/SpeX	2016A076	2016-02-07		5.7	5.0	Protopapa	Protopapa/Kelley
	IRTF/SpeX	2017A076	2017-03-23		2.0	1.4	Protopapa	Kelley
	IRTF/SpeX	2017A076	2017-06-24		1.6	0.9	Protopapa	Protopapa/Kelley
67P/Churyumov-Gerasimenko	IRTF/SpeX	2016A076	2016-02-04	JFC	2.3	1.5	Protopapa	Protopapa/Kelley
	IRTF/SpeX	2016A076	2016-02-07		2.3	1.5	Protopapa	Protopapa/Kelley
PANSTARRS (C/2014 S2)	IRTF/SpeX	2016A076	2016-02-04	OCC	2.2	1.8	Protopapa	Protopapa/Kelley
	IRTF/SpeX	2016A076	2016-02-07		2.2	1.8	Protopapa	Protopapa/Kelley
9P/Tempel 1	IRTF/SpeX	2016A076	2016-04-11	JFC	1.9	1.0	Protopapa	Kelley/Protopapa
	IRTF/SpeX	2016A076	2016-04-12		1.9	1.0	Protopapa	Kelley/Protopapa
100P/Hartley 1	IRTF/SpeX	2016A076	2016-04-11	JFC	2.0	1.1	Protopapa	Kelley/Protopapa
	IRTF/SpeX	2016A076	2016-04-12		2.0	1.1	Protopapa	Kelley/Protopapa
252P/LINEAR	IRTF/SpeX	2016A076	2016-04-11	JFC	1.1	0.1	Protopapa	Kelley/Protopapa
	IRTF/SpeX	2016A076	2016-04-12		1.1	0.1	Protopapa	Kelley/Protopapa
PANSTARRS (C/2014 W2)	IRTF/SpeX	2016A076	2016-04-12	OCC	2.7	2.7	Protopapa	Kelley/Protopapa
	IRTF/SpeX	2016B079	2016-08-12		3.1	3.1	Protopapa	Protopapa
53P/Van Biesbroeck	IRTF/SpeX	2016B079	2016-08-12	JFC	2.6	1.6	Protopapa	Protopapa
Spacewatch (C/2011 KP36)	IRTF/SpeX	2016B079	2016-08-12	OCC	4.9	4.2	Protopapa	Protopapa
41P/Tuttle-Giacobini-Kresak	IRTF/SpeX	2017A076	2017-02-14	JFC	1.3	0.3	Protopapa	Protopapa/Kelley
	IRTF/SpeX	2017A076	2017-03-23	JFC	1.1	0.1	Protopapa	Kelley
	IRTF/SpeX	2017A076	2017-06-24	JFC	1.4	0.4	Protopapa	Protopapa/Kelley
45P/Honda-Mrkos-Pajdusakova	IRTF/SpeX	2017A076	2017-02-14	JFC	1.0	0.09	Protopapa	Protopapa/Kelley
65P/Gunn	IRTF/SpeX	2017A076	2017-06-24	JFC	3.0	2.1	Protopapa	Protopapa/Kelley
71P/Clark	IRTF/SpeX	2017A076	2017-06-24	JFC	1.6	0.6	Protopapa	Protopapa/Kelley
PANSTARRS (C/2016 M1)	IRTF/SpeX	2017A076	2017-06-24	OCC	4.8	4.5	Protopapa	Protopapa/Kelley
29P/Schwassmann-Wachmann 1	IRTF/SpeX	2017A076	2017-06-24	JFC	5.8	5.1	Protopapa	Protopapa/Kelley
C/2015 VL62	IRTF/SpeX	2017A076	2017-06-24	OCC	2.8	2.7	Protopapa	Protopapa/Kelley
PANSTARRS (C/2015 ER61)	IRTF/SpeX	2017A076	2017-06-24	OCC	1.3	1.5	Protopapa	Protopapa/Kelley

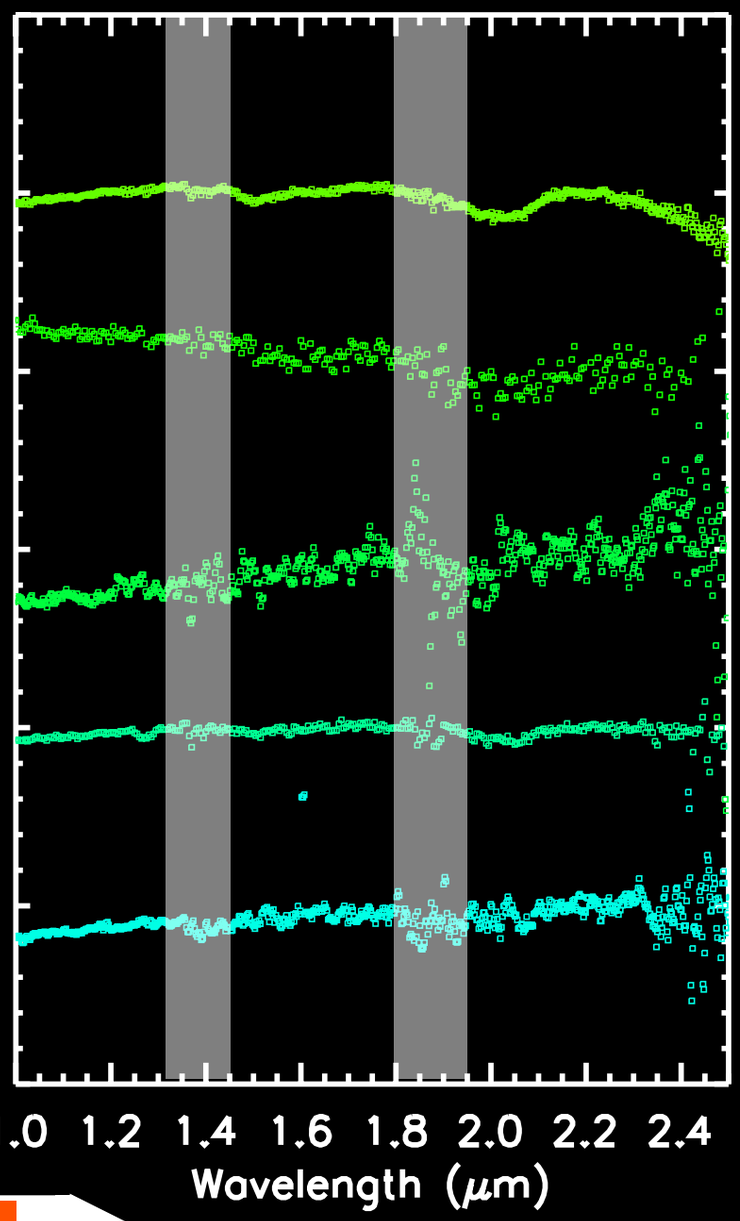
C/2007 N3
C/2013 US10
C/2015 V2
6P/dArrest
29P/SW−1

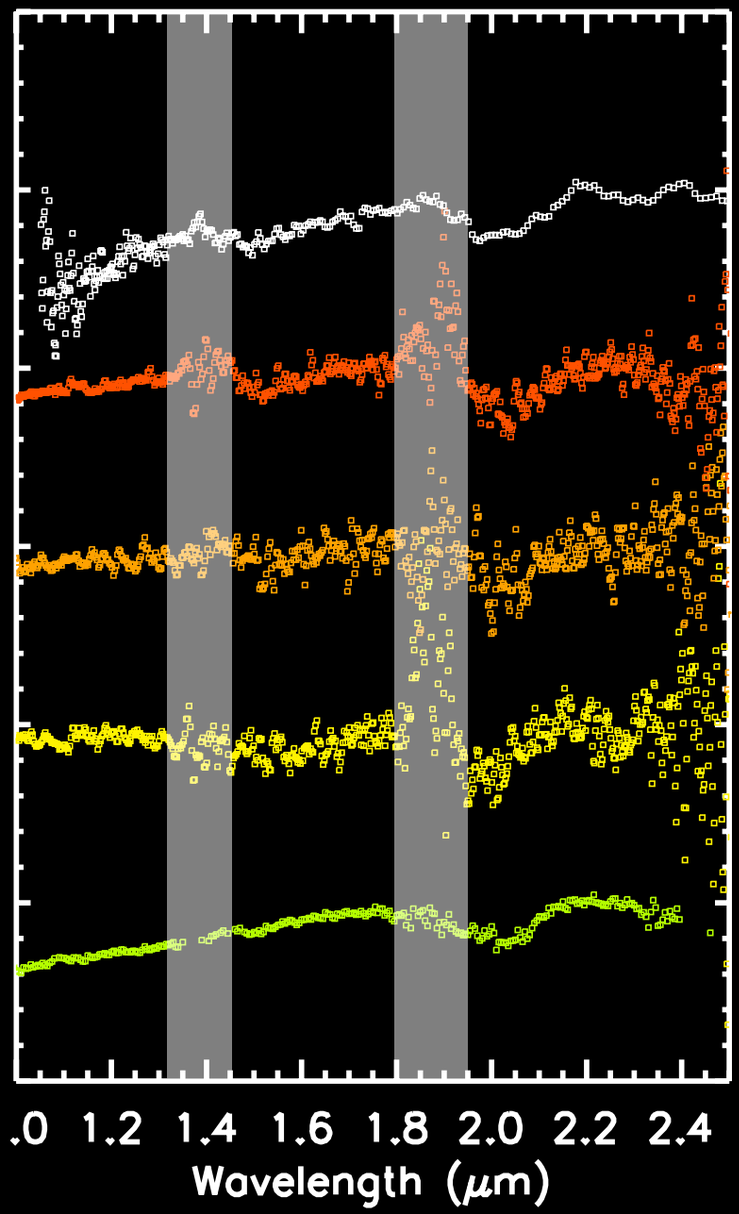
P/2010 H2
C/2005 L3
65P/Gunn
C/2011 L4
117P/Helin−Roman−Alu



103P/Hartley 2
C/2013 US10
C/2013 US10
C/2013 US10
C/2006 W3







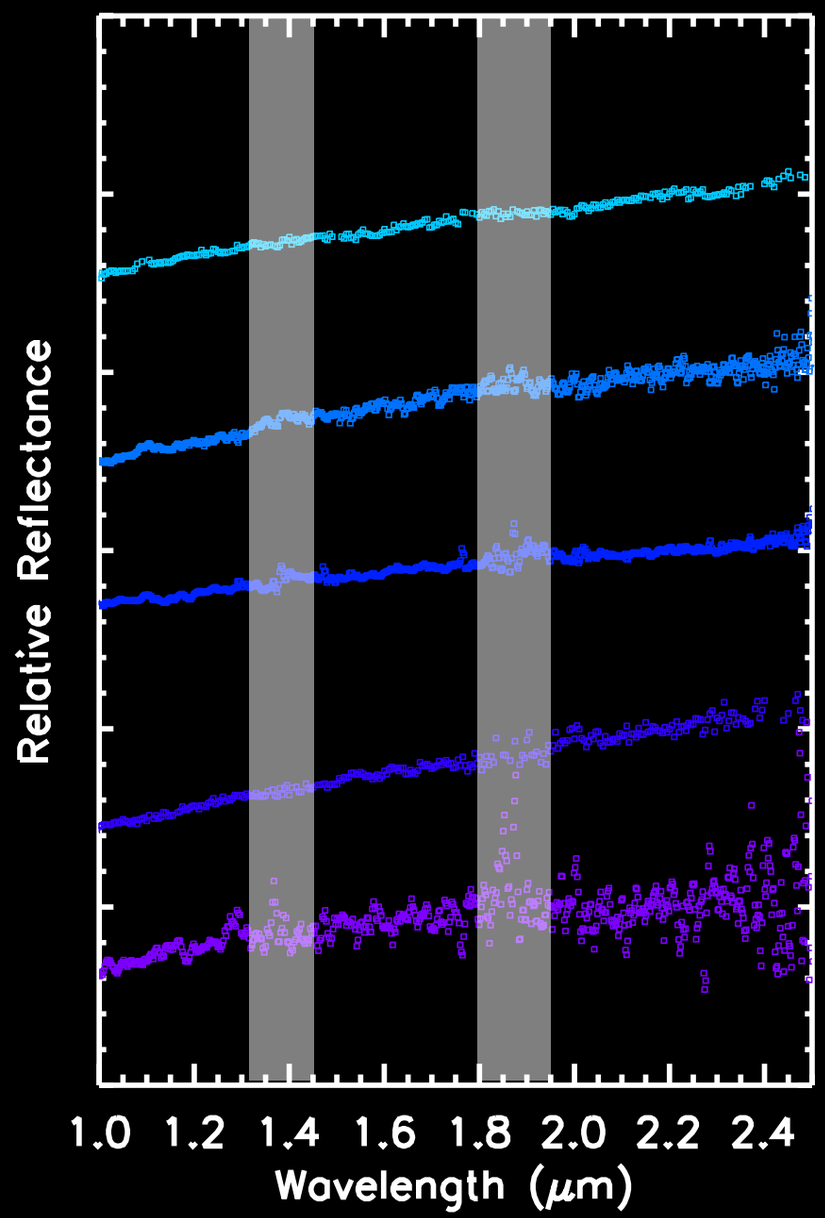


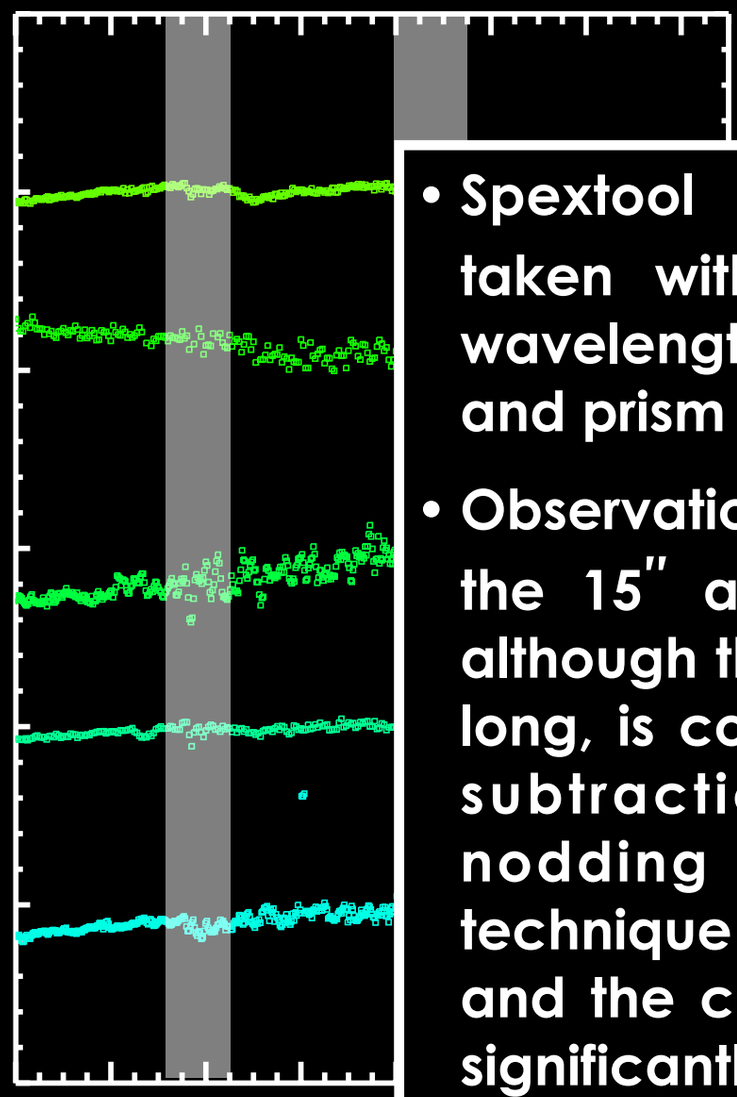
C/2007 N3
C/2013 US10
C/2015 V2
6P/dArrest
29P/SW-1

P/2010 H2
C/2005 L3
65P/Gunn
C/2011 L4
117P/Helin-Roman-Alu



103P/Hartley 2
C/2013 US10
C/2013 US10
C/2013 US10
C/2006 W3

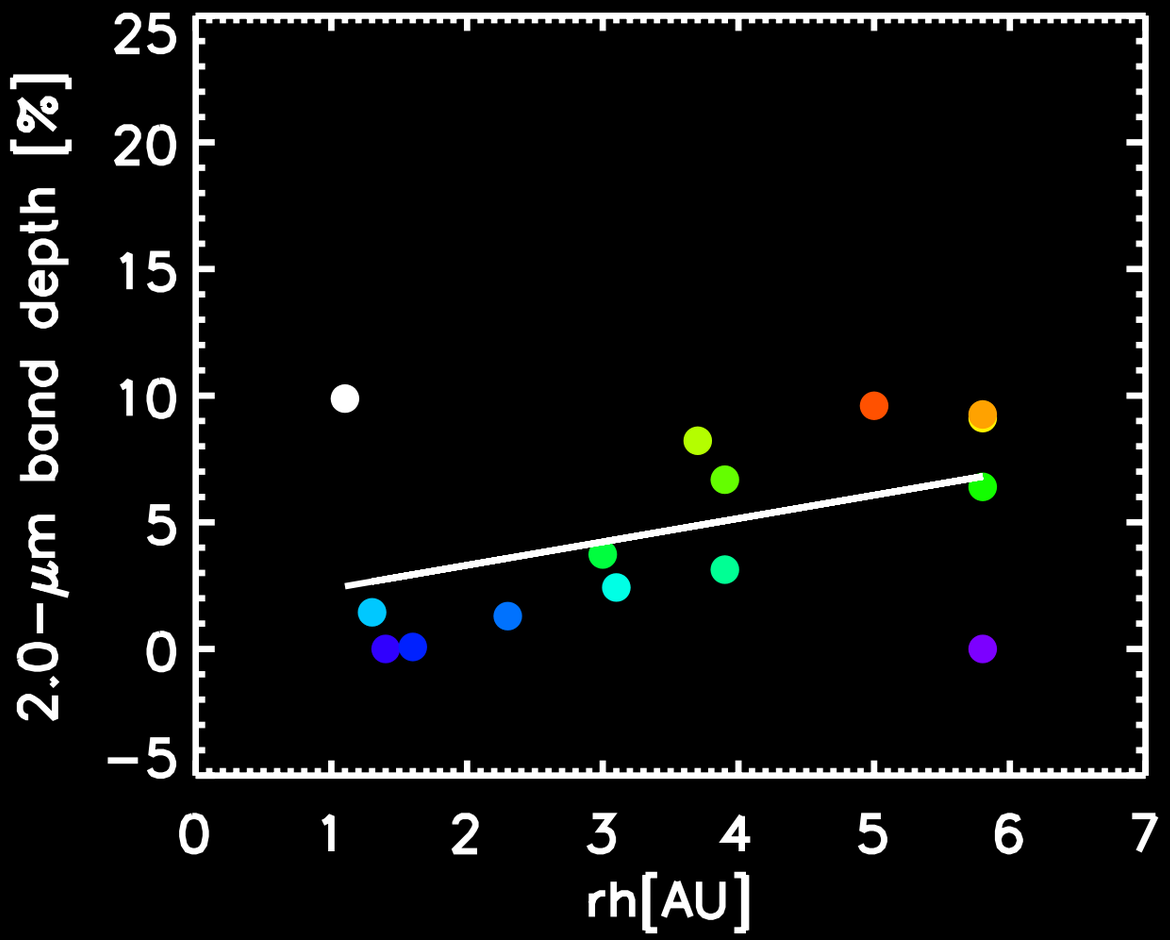




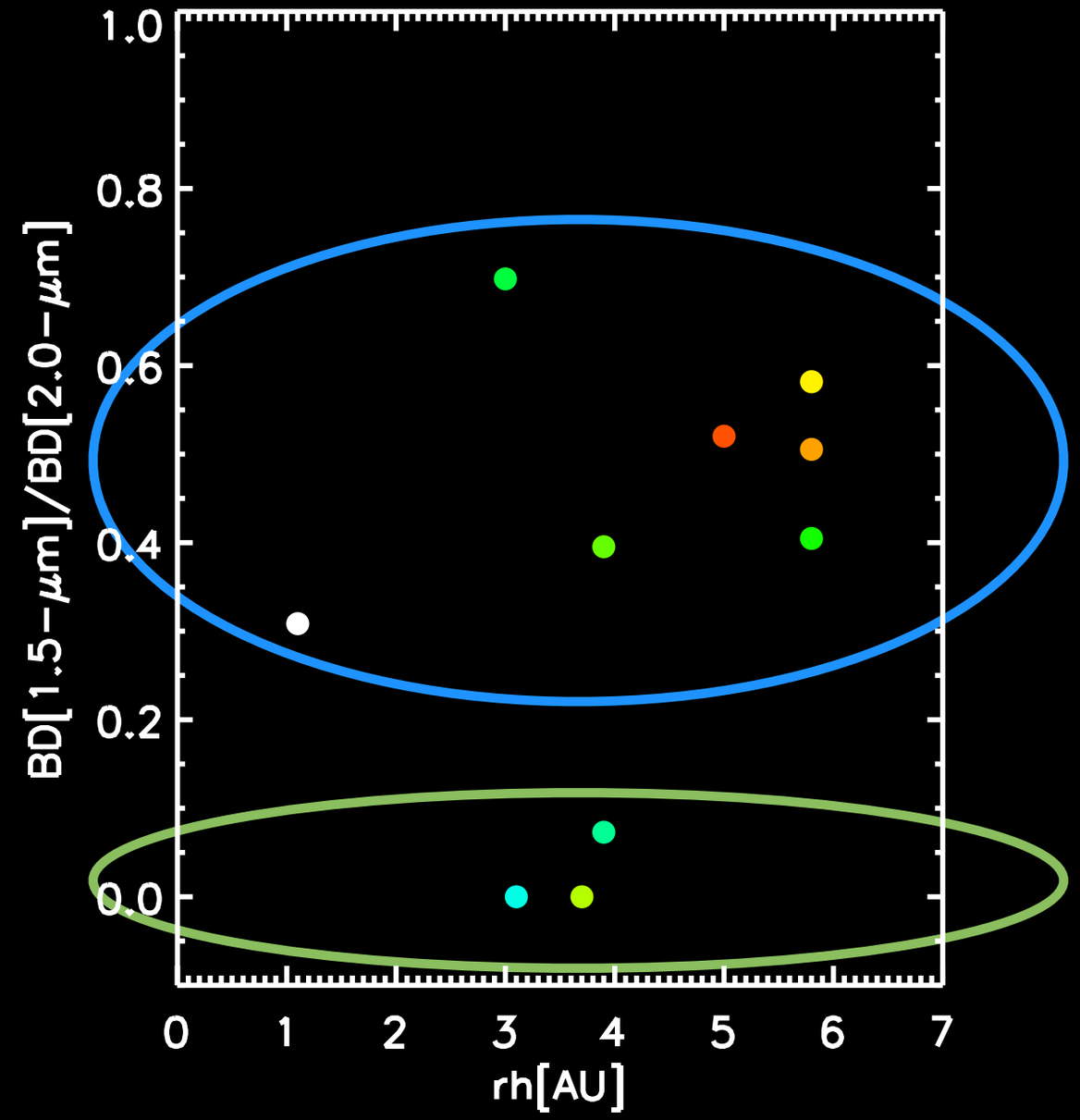


- Spextool was designed to reduce data taken with the 15″-long slit in the short wavelength cross-dispersed (SXD), the LXD, and prism modes.
- Observations of comets were obtained with the 15″ and 60″ slit lengths. The 60″ slit, although there is some curvature for slits this long, is convenient in keeping a clean sky subtraction when the usual A-B-B-A nodding of the target along the slit technique is adopted to acquire the data and the comet is particularly active with a significantly extended coma. I encourage to implement Spextool to reduce data with the 60”-long slit

Preliminary results



The 2.0-μm water-ice band depth presents a positive correlation with heliocentric distance. If the depth of the 2.0-μm band is an indication of water-ice abundance, this trend is not unexpected as heliocentric distance controls the lifetime of the water ice.



The ratio between the depths of the 1.5- and 2.0-μm water-ice absorption bands versus heliocentric distance is shown. This ratio probes the grain size properties of the water ice grains, and reveals two apparent populations in comets: sub-μm-sized (lower group) and μm-sized grains (upper group).

The need of an IRTF South facility

- La Silla Observatory (Atacama desert, Chile)
  - 3.6m telescope
    - HARPS
      fibre-fed high resolution echelle spectrograph
  - NTT
    3.58 m telescope
    (no differential guiding)
    - SofI ("Son of ISAAC", a VLT instrument)
      a near infrared camera and low-resolution spectrograph

      EFOSC2
      Optical Faint Object Spectrograph and Camera
  - 2.2 m telescope
    - FEROS
      The Fiber-fed Extended Range Optical Spectrograph

      WFI
      Wide Field Imager
- Cerro Tololo Inter-American Observatory (La Serena, Chile)
  - Victor M. Blanco Telescope
    4 m telescope
    - ARCoIRIS is an infra-red imaging spectrograph
      COSMOS: visible Multi-Object Spectrograph
      DECam high-performance, wide-field CCD imager
  - Southern Astrophysical Research (SOAR)
    4.1 m telescope
    - SPARTAN Near-IR Camera
      OSIRIS: IR Imager/Spectrograph no longer available

Important for analysis of statistical sample:

- Double the target sample
- Guarantees a systematic comparison between data acquired from the N and S facilities
- No facilities available in the South with similar capabilities as those at IRTF

SpeX modes



PRISM 0.7-2.52 micron, R~200 matched to 0.3x15" slit or 0.3x60" slit

SXD 0.7-2.55 micron, R~2000 matched to 0.3x15" slit

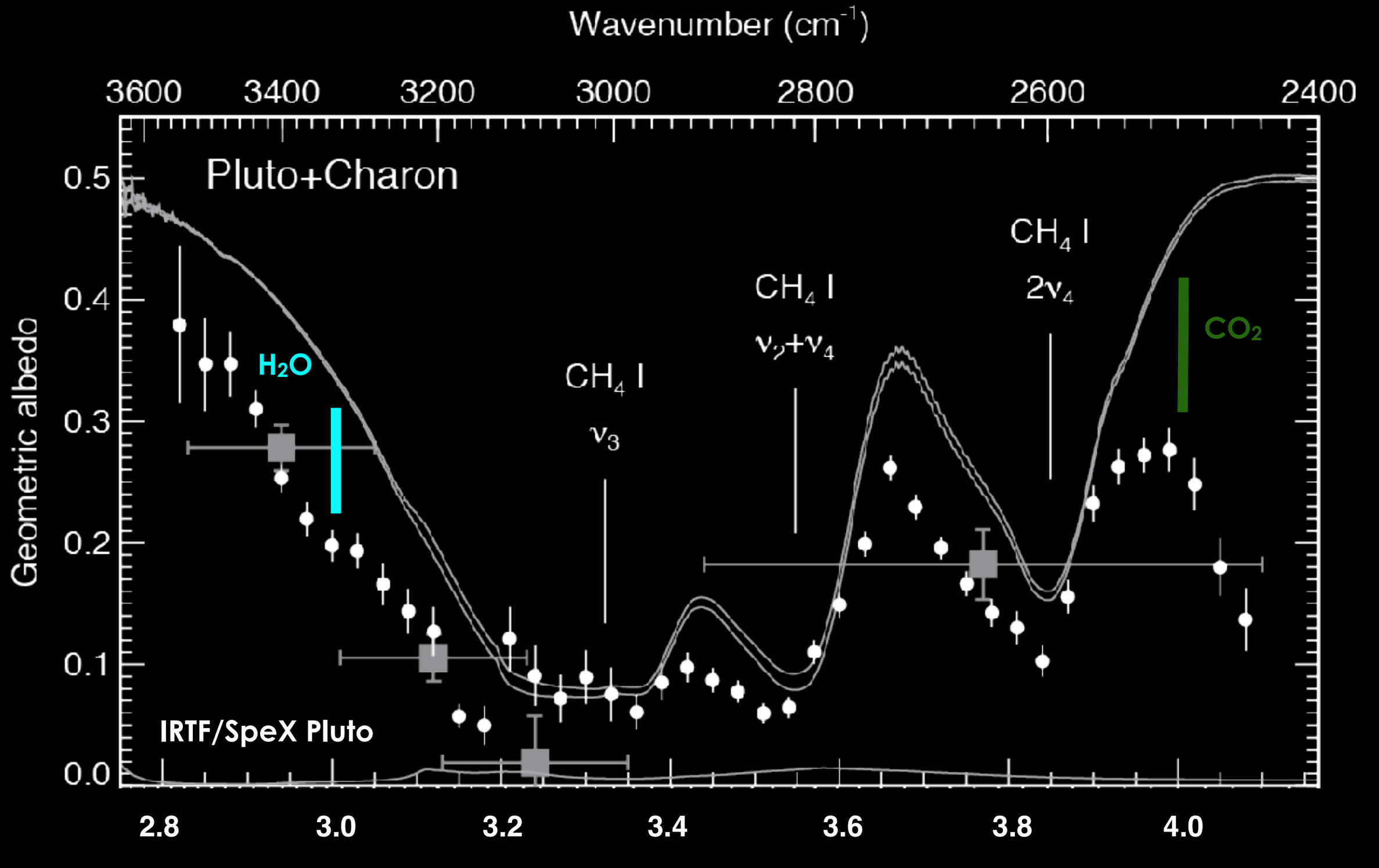
LXD_short 1.67-4.2 micron, R~2500 matched to 0.3x15" slit

LXD_long 1.98-5.3 micron, R~2500 matched to 0.3x15" slit

Suggestion:
PRISM 0.3-4.2μm R~200

L- band ground-based data

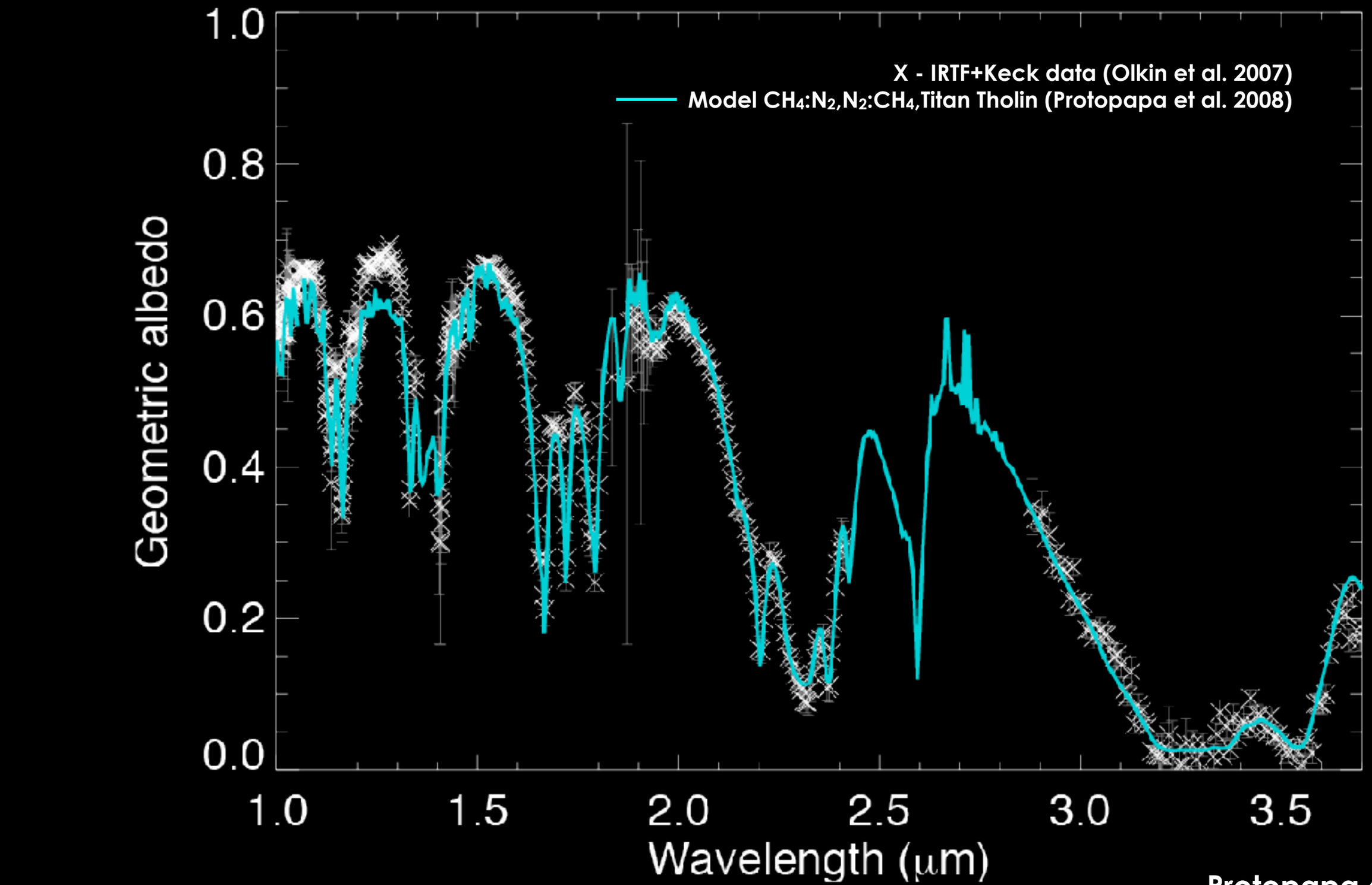




2–4 μm cross-dispersed mode of SpeX

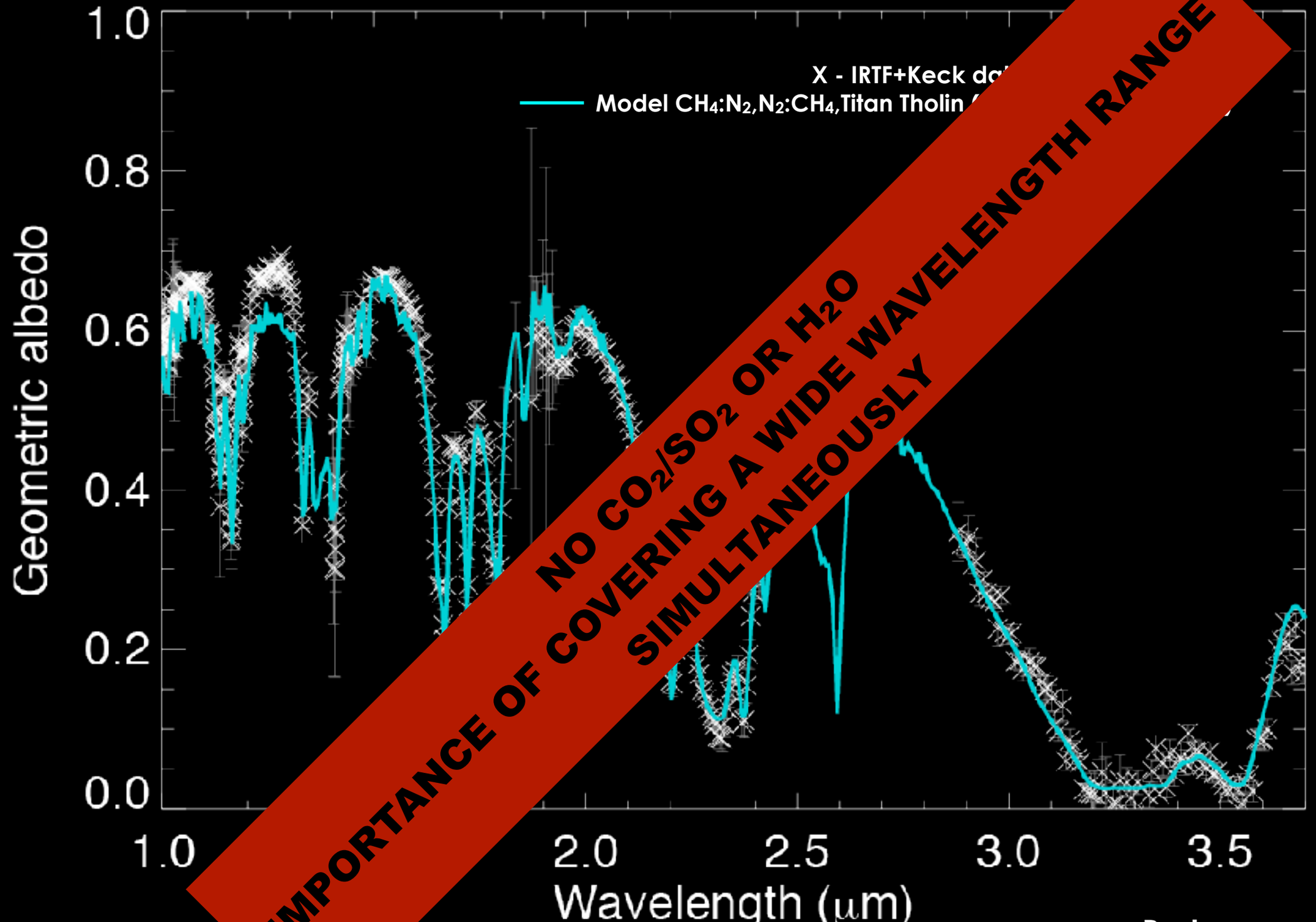
Grundy, Buie, Spencer, 2002

L- band ground-based data



Protopapa et al. 2008

L- band ground-based data



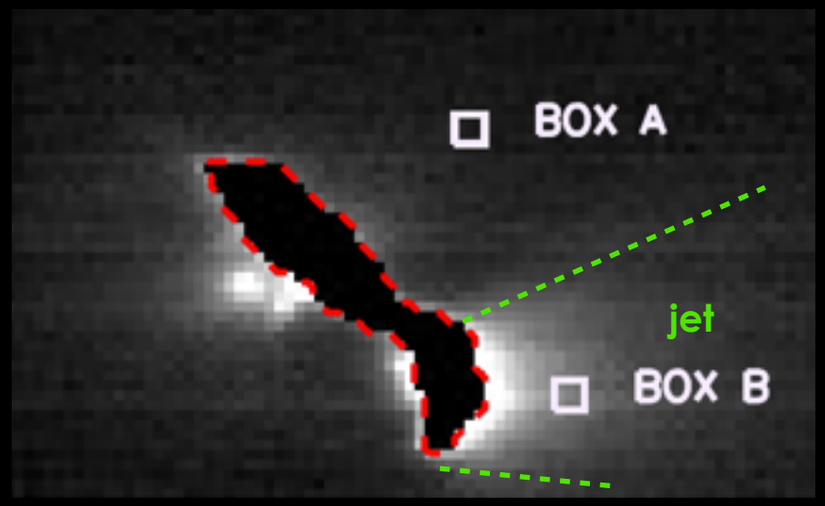
IMPORTANCE OF COVERING A WIDE WAVELENGTH RANGE SIMULTANEOUSLY

NO CO_2/SO_2 OR H_2O

Protopapa et al. 2008

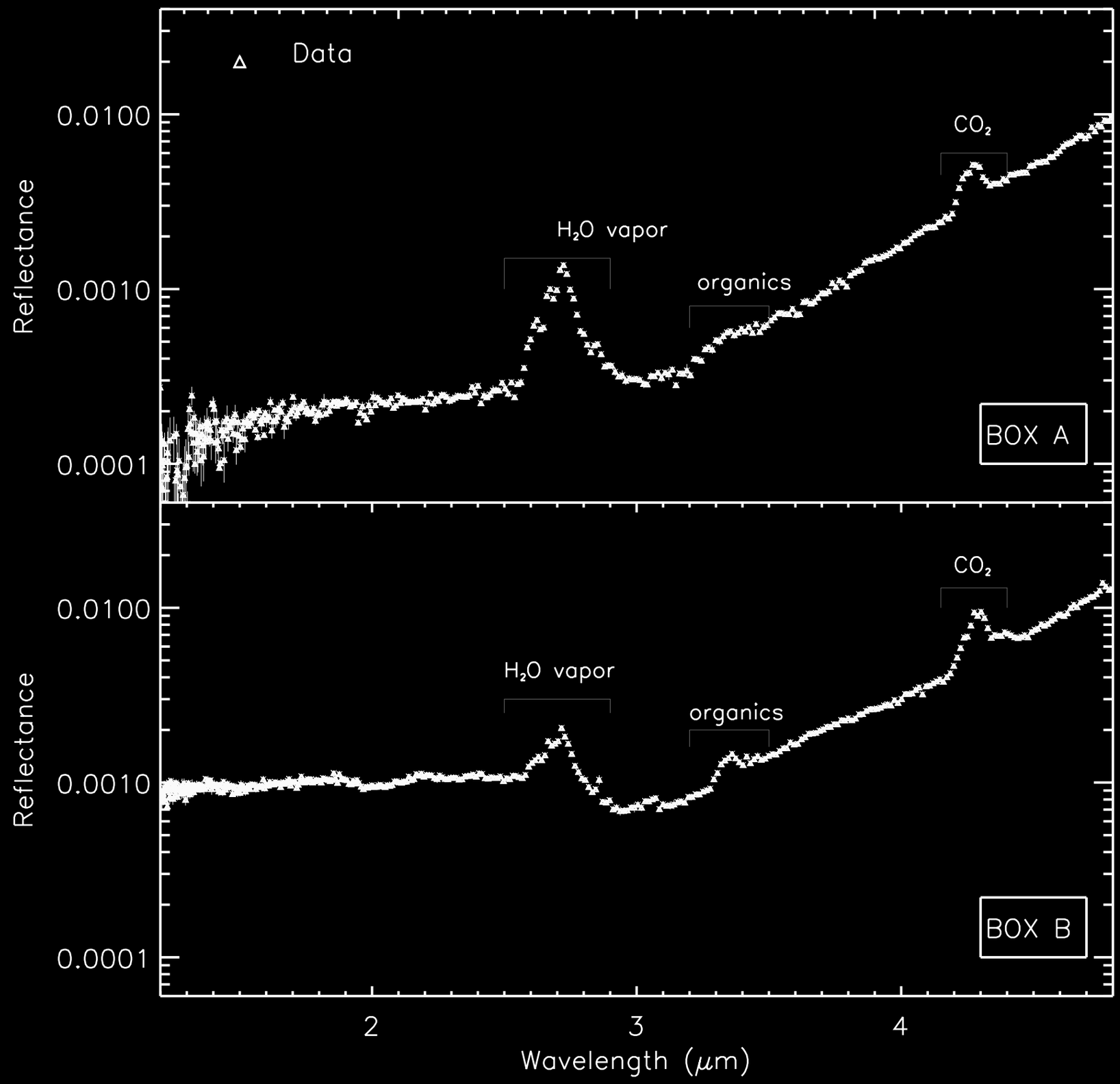
The use of IFU

Protopapa et al., 2014



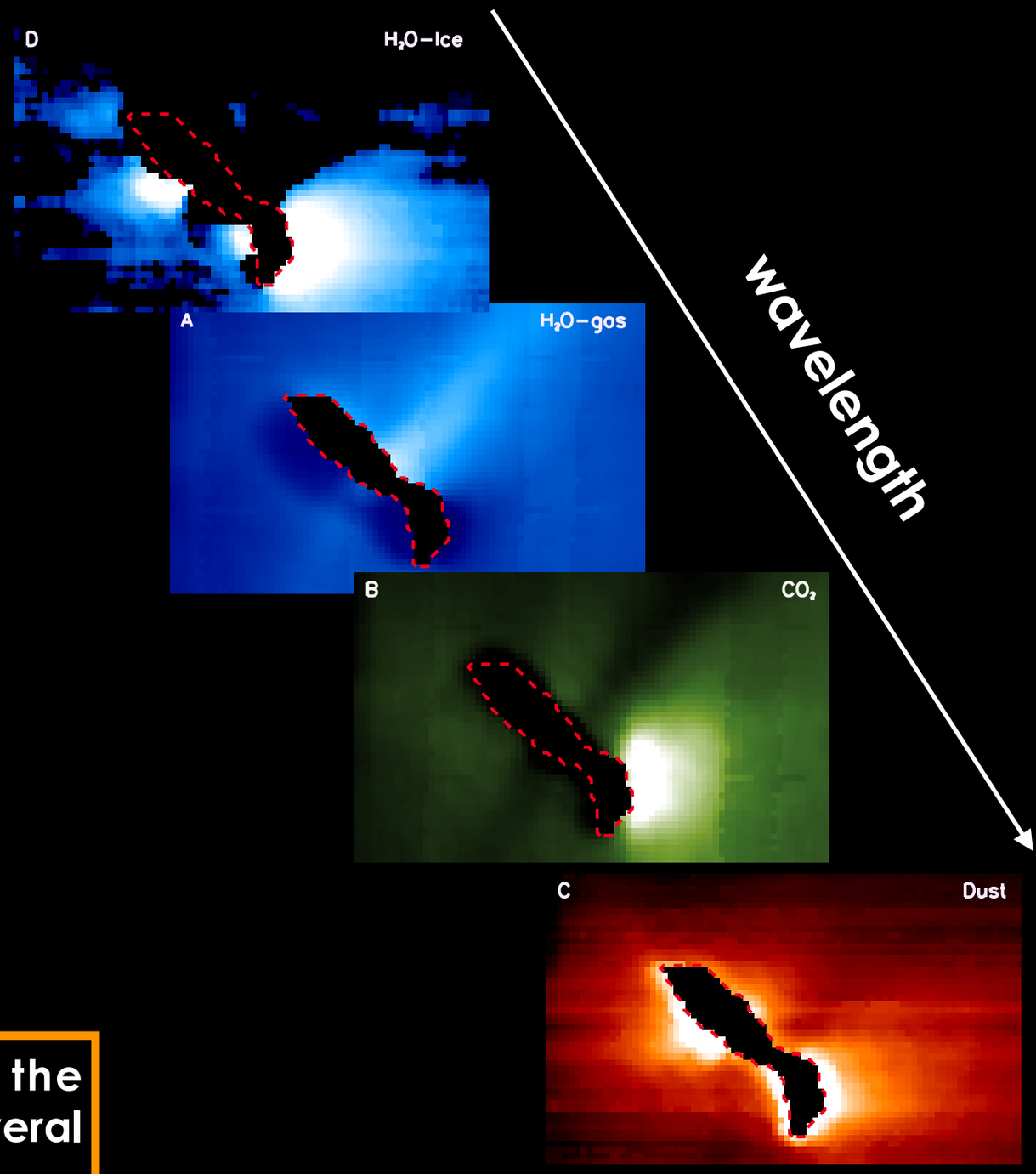
Deep Impact HRI-IR spatially resolved spectra of comet 103/P Hartley 2 (The IR imaging spectrometer operates from 1.05 to 4.80 μm with a spectral resolving power (λ/λ) that varies from a minimum of 200 at middle wavelengths to higher values at shorter and longer wavelengths.

- Red slope in the range 1.0-2.5 μm
  - refractory component (amorphous carbon)
- Sharp rise beyond 2.5 μm
  - thermal emission from the hot dust in the coma
- The spectra extracted in the jet regions present absorption bands at 1.5, 2.0, and 3.0 μm



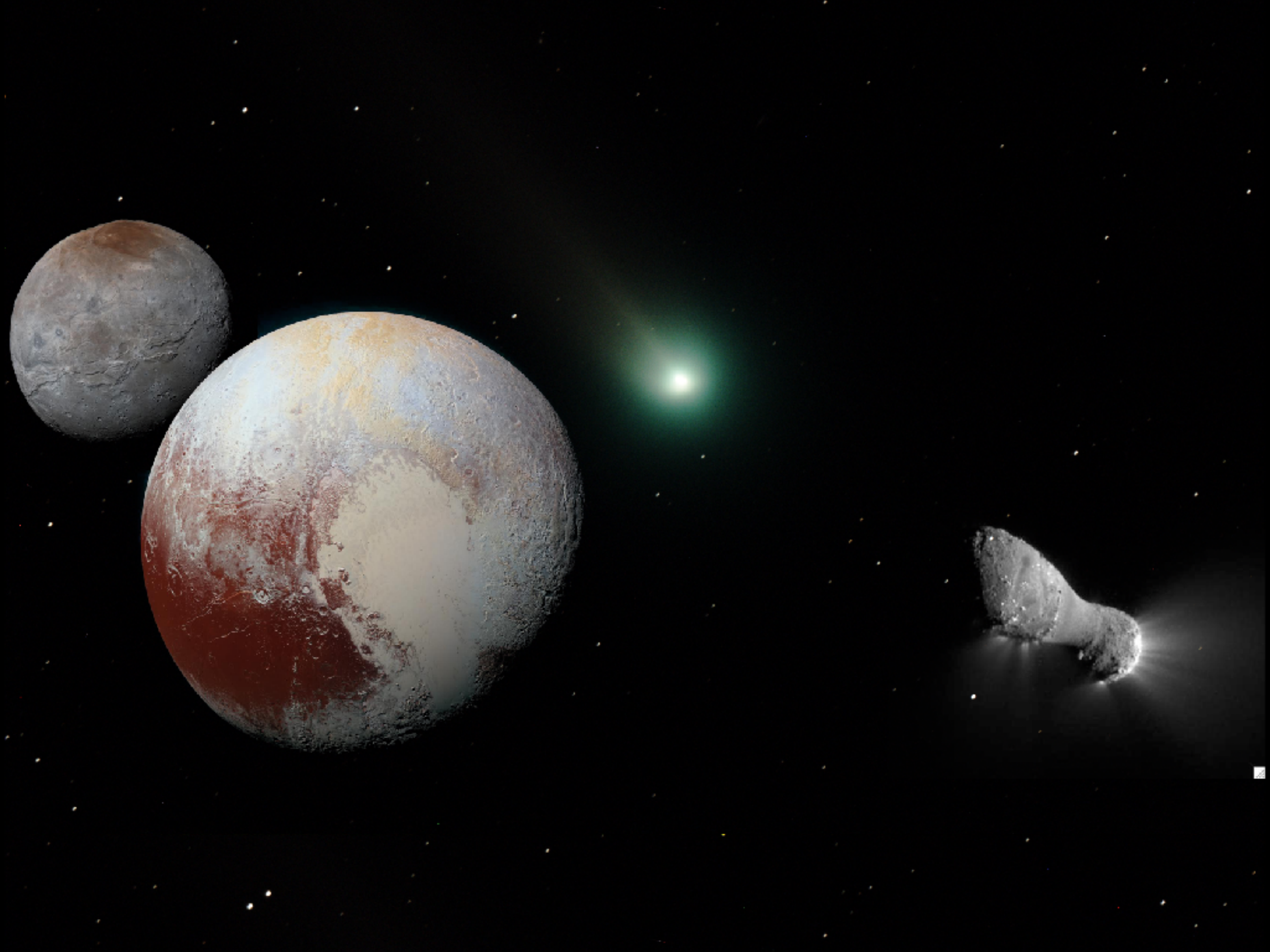
The use of IFU





Spectroscopically map the spatial distribution of several species in the coma

Protopapa et al., 2014



Thank you!